THESIS

EVALUATING AND CORRECTING SENSOR CHANGE ARTIFACTS IN THE SNOTEL TEMPERATURE RECORDS, SOUTHERN ROCKY MOUNTAINS, COLORADO

Submitted by

Chenchen Ma

Department of Ecosystem Science and Sustainability

In partial fulfillment of the requirements

For the Degree of Master of Science

Colorado State University

Fort Collins, Colorado

Summer 2017

Master's Committee:

Advisor: Steven Fassnacht
Co-Advisor: Stephanie Kampf

Yu Wei

ABSTRACT

EVALUATING AND CORRECTING SENSOR CHANGE ARTIFACTS IN THE SNOTEL TEMPERATURE RECORDS, SOUTHERN ROCKY MOUNTAINS, COLORADO

In many high elevation mountain regions, documented warming rates have been greater than the global surface average. These warming rates directly affect the snowpack, runoff, ecosystems, agriculture and species that rely on a high elevation snowpack. Temperature records from the snow telemetry (SNOTEL) network across the Southern Rocky Mountains in the western United States have high warming rates, which may have been affected by systematic inhomogeneities in the temperature data caused by sensor changes. This study evaluates the maximum, average, and minimum temperature trends from 68 long-term SNOTEL stations across Colorado for the period from the 1980s through 2015 using the non-parametric Mann-Kendall/Theil-Sen's analyses before and after the temperature records were corrected for the sensor-caused inhomogeneities. Three homogenization methods were tested using a simple temperature index snow accumulation and melt model.

Results show that the significant warming trends found in the original datasets, especially in minimum temperature (average increase of 1.2 °C per decade), decreased (to an average of 0.5 °C per decade) after homogenization. Step-like shifts in temperature datasets were observed in SNOTEL temperature records at the time of temperature sensor change, which created a discontinuity in the temperature dataset. The temperature-index snow model simulated snow water equivalent (SWE) well (more than 93% of the calibrated stations within the "good" and "very good" performance category for all three statistical-evaluation periods based on the Nash-

Sutcliffe coefficient of efficiency, NSCE) using the new temperature sensor dataset. However, these models did not perform as well when using the original (pre-sensor change) and homogenized temperatures, with 23% of stations for the original temperature data and 44-69% of stations for two homogenized temperature datasets within the “good” and “very good” performance categories. The homogenized temperature records simulated snow water equivalent (SWE) better than the original uncorrected temperature data, but they did not fully correct for the effects of sensor change on the temperature records. The NSCE and bias statistics from SWE modeling using the original and homogenized datasets suggest that the homogenization methods evaluated in this study are applicable for many of the SNOTEL stations in Colorado but not all, and need to be applied with caution. Potential users of temperature products from the SNOTEL network should also be very careful when choosing time periods for future climate change research and assessments. More long-term climate monitoring stations should be installed in high elevation mountain regions to document and investigate elevation-dependent warming.

ACKNOWLEDGEMENTS

First and foremost, I would like to thank my advisor and my co-advisor, Drs. Steven Fassnacht and Stephanie Kampf, for their constant patience and guidance through my undergraduate and master's degree. I would also like to thank my committee member Dr. Yu Wei for his contributions to my thesis and my graduate education. This research was partially funded by Colorado Water Conservation Board (CWCB). In addition, I would like to thank the Department of Ecosystem Science and Sustainability at CSU. I would also like to express my gratitude to Dr. Jared Oyler for providing the homogenized temperature data. Finally, I am very thankful to my family and friends for their endless support through my education and life.

TABLES OF CONTENTS

CHAPTER 1: INTRODUCTION

Global mean surface temperature increased 0.85°C from 1880 to 2012 (IPCC, 2014). Since 1975, two-thirds of the warming has occurred at an approximate rate of 0.15-0.2°C per decade (Hansen et al., 2010). There is growing evidence that the rates of warming at high elevations are greater than the global land average (Rangwala and Miller, 2012; Pepin et al., 2015). Multiple studies from different mountain regions in the world have documented elevation-dependent warming, where temperature trends at high elevations are generally greater than those at lower elevations (Liu et al., 2009; Diaz and Eischeid, 2007; Clow, 2010; Harpold et al., 2012; Rangwala and Miller, 2012; Yan and Liu, 2014; Pepin et al., 2015).

Documented temperature trends in the Tibetan plateau are 0.42°C per decade for the annual mean temperature from 116 meteorological stations at an elevation higher than 2000m (Liu et al., 2009). In this same region, Yan and Liu (2014) found warming rates of 0.36 and 0.50°C per decade for locations over 3000 m and over 4000 m respectively, especially from 2001 to 2012. These warming rates are similar to those reported for the Swiss Alps, where Ceppi et al. (2012) found an annual average warming rate of 0.35°C per decade. In addition, available observations suggested that the Colorado Rocky Mountains in the western U.S. were experiencing greater seasonal warming rates (0.50-1.0°C per decade) than lower elevations during the last three decades, particularly since the mid-1990s. These trends were determined based on long-term annual mean temperature from the SNOTEL network (Clow, 2010; Pederson et al., 2011; Harpold et al., 2012; Rangwala and Miller, 2012; IPCC, 2014).

Understanding the warming patterns in regions of high elevation is important because it directly affects the snowpack, runoff, ecosystems, agriculture, and species that rely on high

elevation habitats (Pepin et al., 2015). Only a few studies have addressed the possible reasons for elevation-dependent warming, which include snow-albedo feedback, cloud properties, water vapor, and radiative fluxes (Rangwala and Miller, 2012; Pepin et al., 2015). In the Colorado Rocky Mountains in the western U.S., where some of the greatest rates of warming have been reported, there is evidence that temperature trends are affected by systematic data artifacts due to sensor inhomogeneities, defined as "*non-climatic temperature jumps and trends resulting from changes in observation protocols, instrumentation, or station siting*" (Oyler et al., 2015). These inhomogeneities are present in data from the Natural Resources Conservation Service (NRCS) Snow Telemetry (SNOTEL) network <*wcc.nrcs.usda.gov*>. There are more than 800 SNOTEL stations located at high elevation stations across the western United States that have been recording data for about 30 years <*http://www.wcc.nrcs.usda.gov/about/prog_overview.html*>.

1.1 The SNOTEL Dataset

The automated SNOTEL monitoring network, operated by the Natural Resources Conservation Service (NRCS), was initially designed as a water supply forecasting hydro-climatic data collection network in the late 1970's to complement and replace existing manual snow courses (Julander et al., 2007). Snow water equivalent (SWE), snow depth, and density were measured at the snow courses, typically on the first of the month over the winter (from February through May in Colorado). The SWE data were used to forecast seasonal runoff volumes in mountain rivers. To that end, locations of the SNOTEL stations were specifically chosen for forecasting water supply in the western United States.

During the mid 1980's, daily minimum, average, and maximum air temperature data were added to standard data collection but without any uniformity in mounting temperature sensors and measurement protocols (Julander et al., 2007). Hence, these temperature

measurements had less consistency and less quality control compared to precipitation and SWE measurements made from the onset of the establishment of the SNOTEL network (Julander et al., 2007; Rangwala et al., 2015). Initially, YSI temperature sensors were used to record temperature data at or near the SNOTEL data logging hut. In the late 1990s to mid-2000s, several sensor changes were made as follows: i) the sensor was changed from a (standard) YSI to a YSI Extended Range sensor <ysi.com>, ii) the radiation shield was changed, iii) the voltage to temperature algorithm was changed, and iv) the sensor location was changed so that all are now at the same relative position, on a cross-arm off the tower opposite the snow pillow and snow depth sensor (Julander et al., 2007). Unfortunately, the original temperature sensor configuration was only maintained concurrently with the new configuration at a few stations in Idaho. This temperature sensor change has caused inhomogeneities in the historical temperature observations in SNOTEL network across Colorado.

Oyler et al. (2015) evaluated SNOTEL minimum and maximum temperature observations from 1991- 2012 compared to the U.S. Historical Climatology Network (USHCN). They developed a pairwise homogenization algorithm, which identifies and removes relative inhomogeneities in the historical temperature records by comparing station temperature series to stations in the surrounding area (Menne and Williams, 2009; Oyler et al., 2015). They computed trends using an ordinary least squares linear regression on time series of annual temperature anomalies and showed substantial biases in trends at SNOTEL stations, especially for minimum temperature across the Southern Rocky Mountains of Colorado (Oyler et al., 2015 Figures 2e, 2f, S3e, and S3f). Results from their research showed that the minimum temperature trend from 1991-2012 was 1.16°C per decade before applying the homogenization algorithm and reduced to

0.11°C per decade after homogenization. Homogenization made the high elevation SNOTEL temperature trends statistically indistinguishable from lower elevation trends (Oyler et al., 2015).

However, trends computed by Oyler et al (2015) from the adjusted SNOTEL temperature dataset are not consistent with trends over a similar time period (1989 to 2008) from an elevation gradient in the Front Range in Colorado (McGuire et al., 2012). Moreover, Oyler's adjustments tend to create too uniform trends (Figure 1a-b), especially compared to the sets of pre and post-sensor change trends (Figure 1c-d).

In relatively flat terrain, such as the Eastern Plains of Colorado (Pielke et al., 2002) and the Northern Great Plains (Fassnacht et al., 2016), temperatures (and other climatic trends) are often different, even over short distances. Therefore, it is still unclear how well the Oyler et al. (2015) homogenization method works in the study area.

1.2 Questions and Objectives:

In this research, the overall research questions are: 1) How do temperature sensor changes in SNOTEL stations affect temperature trends at SNOTEL stations across the state of Colorado? and 2) Can the inhomogeneities in temperature observations be corrected? To address these questions, the objectives are as follows: 1) Test three different homogenization methods that attempt to correct temperature data biases due to the change of sensors. These methods are: (H1) a bias correction based on co-located old and new temperature sensors in Idaho, (H2) adjustment values provided by the Oyler et al. (2015) study, and (H3) pairwise comparisons between SNOTEL stations in Colorado and nearby Global Historical Climatology Network - Daily (GHCN-Daily) <*https://www.ncdc.noaa.gov/cdo-web/search*>, 2) Compare warming trends derived from homogenization methods versus those derived from the original SNOTEL temperature records, and 3) Examine the performance of different temperature homogenization

methods by modeling Snow Water Equivalent (SWE) with a temperature index snow accumulation and melt model. This objective provides an independent test of the temperature homogenization methods. The modeling performance is statistically evaluated for three periods per year: all days, snow months only (October through June), and melt months only (March through May).

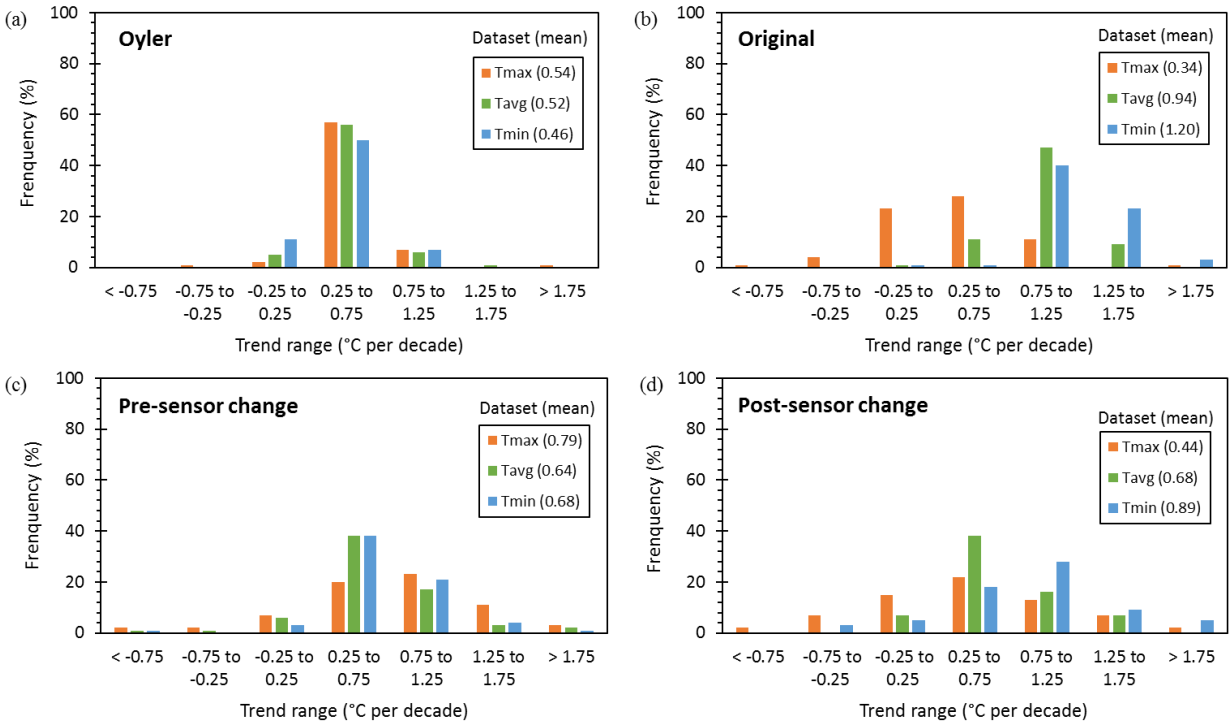

Figure 1. Histogram of Colorado SNOTEL temperature trends derived from (a) Oyler et al. (2015) temperature homogenization method from 1980s to 2015, (b) Original temperature data from 1980s to 2015, (c) Pre-sensor change temperature data from 1980s to 2006, and (d) Post-sensor change temperature data from 1998~2006 to 2015.

CHAPTER 2: DATA AND METHODS

2.1 Study Region and Stations

The study area is the Southern Rocky Mountains in Colorado (Figure 2). This area is the source of four major rivers: the Arkansas, the Colorado, the Platte, and the Rio Grande (Colorado Water Conservation Board, 2015). The steep mountain topography creates dramatic local temperature differences and complex precipitation patterns. Annual average precipitation in the southern Rocky Mountain region ranges from 200 to 1500mm (Doesken et al., 2003). Rain dominated precipitation occurs at area with elevations lower than around 2300m, whereas snow dominated precipitation occurs at all higher elevations (Kampf and Lefsky, 2015). Snow that persists throughout the winter (seasonal snow) covers approximately 26 percent of the area in Colorado. Seasonal snow is found at elevations as low as 2286m in the northwestern part of the state (Kampf and Fassnacht, 2016). Most seasonal snow at the Southern Rocky Mountains in Colorado starts to accumulates in October, and peak accumulation time varies from March through June (Kampf and Fassnacht, 2016)

This study uses the 68 long-term SNOTEL stations in Colorado with at least 25 years of record (from Fassnacht and Records, 2015) (Figure 2). The elevations of study stations range from 2560m (Dry Lake, north-east of Steamboat Springs) to 3536m (Beartown, located in the San Juan Mountains near Silverton). All stations experience seasonal snow cover, and most of them are located in the persistent snow zone (Moore et al., 2015). The northern-most SNOTEL station is located in Larimer County at 40°53’ N while the southern-most SNOTEL is located in Conejos County at 37°01’ N. The physical distance between SNOTEL stations ranges from 2.1km (Kiln to Nast Lake) to 430km (Roach to Cumbres Trestle). Tower is the SNOTEL site that

has the largest mean maximum SWE of 1324mm and is located on Buffalo Pass near Steamboat Springs, Colorado. The SNOTEL station with the smallest mean maximum SWE of 144mm is Copeland Lake, located in Rocky Mountain National Park near Allenspark, Colorado.

2.2 Dataset

From all selected SNOTEL stations, we downloaded daily maximum, average, and minimum air temperature, precipitation, and Snow Water Equivalent (SWE) data from the NRCS website <*http://www.wcc.nrcs.usda.gov/snow/*>. Station records range from the early 1980s to 2015. Most of the temperature sensor changes in the state of Colorado occurred from the late 1990s to mid-2000s; all temperature data were divided into two time periods, pre-sensor change and post-sensor change. The temperature time series after the sensor change (starting from1998 to 2006) was assumed to be correct, and homogenization methods were applied to adjust the pre-sensor change data to the post-sensor change data (Domonkos, 2016).

2.3 Temperature Data Quality Control

To remove observation errors and invalid values from temperature dataset, all SNOTEL stations were divided into four major clusters based on their longitude and latitude. Nearby stations that are experiencing similar precipitation variability and climate patterns were considered as one group according to a climate cluster map (Figure 2), which was derived through multivariate statistical techniques include clustering and rotated Principal Components (Wolter, 2001). Although climatic trends from adjacent stations can vary in magnitude and direction (Pielke et al., 2002; Fassnacht et al., 2016), the comparison of temperature records to other stations facilitated temperature data quality evaluation. Maximum, average, and minimum temperature data from all SNOTEL stations in one of the four climate clusters were plotted from 1985 to 2015 by group to search for obvious anomalies such as "*physically impossible or*

climatologically implausible temperature values for the locations and time of the year" (Durre et al., 2010), which indicate sensor error. Temperature values in each group that were abnormally higher or lower (> three standard deviations) than all neighboring stations were removed. Other anomalies such as temperature values that do not vary for several weeks or months or gradually varying values that are not consistent with other stations were also removed.

Many previous studies have used non-missing neighboring observations to infill missing data at a target station and create serially complete station data (DeGaetano et al., 1995; Huth and Nemesova, 1995; Eischeid et al., 2000; Oyler et al., 2015). For each station, a best fit linear equation was derived to relate the target station daily temperature to the mean temperature from all other stations in the same group. These equations had average R^2 values of 0.95 (minimum temperature) to 0.98 (average temperature) and were used to infill the target's missing values. The amount of filled values ranges from 4.4% to 11.1% of the daily records for average temperature, 6.1% to 22.2 % for maximum temperature and 7.8% to 13.4% for minimum temperature.

2.4 Homogenization Approaches

Three approaches were applied to correct the temperature imhomogeneities at the SNOTEL station, leading to three adjusted temperature datasets (Table 1).

2.4.1 H1 (Morrisey Concurrent Observations)

The first temperature homogenization method (H1) was derived from four SNOTEL stations in Idaho, where data from the old sensors and new sensors were collected concurrently from 1999 to 2001 and were compared to explore the apparent cold temperature bias for the old sensors (data from Phil Morrisey, hydrologist, USDA NRCS shown in Figure S4 of Oyler et al.,

2015). The H1 adjustment equation (Equation 1) is the best-fit curve for the Morrisey concurrent data using a fourth-order polynomial, as follows:

$$T_{adjusted} = 5.30 \times 10^{-7} T_{old}^4 + 3.72E \times 10^{-5} T_{old}^3 - 2.16 \times 10^{-3} T_{old}^2 - 7.32 \times 10^{-2} T_{old} + 1.37 \quad \text{(Equation 1)},$$

where $T_{adjusted}$ is the revised H1 temperature in degrees Celsius (deg. C), and T_{old} is the original temperature from the period before the sensor change in deg. C. This equation (Equation 1) was applied to the pre-sensor change quality-controlled and filled average temperature datasets.

2.4.2 H2 (Oyler's Temperature Adjustments)

Oyler et al. (2015) provided corrections to the daily minimum and maximum SNOTEL dataset (482 stations total including the 68 study stations) based on comparisons to the U.S. Historical Climatology Network (USHCN, see Menne et al., 2009) dataset (320 stations) over the period from 1991 to 2012. For each SNOTEL station, they provide either one or several adjustment values, which can be added or subtracted from every daily temperature value. If more than one adjustment value is provided, each value applies to a specified range of dates. All adjustment values obtained from Oyler et al. (2015) for each study site were applied to the daily filled original maximum and minimum temperature datasets by adding or subtracting the adjusted values. Average daily temperature values were then computed as the mean of the daily adjusted maximum and minimum temperature datasets.

2.4.3 H3 (GHCN-D Pairwise Method)

The GHCN (Global Historical Climatology Network)-Daily is an integrated database that contains daily climate summaries from over 75,000 surface stations across the globe (Burroughs, 2009). In this study, five GHCN-D sites in Colorado were paired with nearby SNOTEL stations. These pairs were: Yampa with Crosho, Glenwood Springs #2 with Bison Lake, Climax with

Fremont Pass, Aspen #1 SW and Leadville Lake CO Airport with Kiln. The GHCN-D sites were selected because they are adjacent to the listed SNOTEL study stations within distances ranging from 1.7 km to 27.4 km (Figure 2). Maximum and minimum temperature data from each site for the period 1980 to 2015 were downloaded directly from National Oceanic and Atmospheric Administration (NOAA) <*https://www.ncdc.noaa.gov/cdo-web/*>. Temperature data from all GHCN-D sites were aligned with SNOTEL datasets because there were missing dates in the GHCN-D system. Aspen #1 SW and Leadville Lake CO were aligned and averaged as one dataset because their distances to Kiln SNOTEL site are about the same, and it is more comprehensive to group them as one dataset. The two datasets from the post-sensor change period of GHCN-D and SNOTEL were then plotted as scatter plot, and the best fit line was determined using linear regression. The derived equation for each SNOTEL station was then applied to the pre-sensor change period to get daily H3 maximum and minimum temperature datasets. Daily average temperature values were then computed from the daily H3 maximum and minimum temperature datasets. These steps were applied to all four SNOTEL stations with their paired GHCN-D sites.

2.5 Trend Analysis

To investigate annual temperature trends in each of the datasets from all SNOTEL stations, a Mann-Kendall non-parametric trend analysis was conducted (Mann, 1945; Kendall and Gibbons, 1990). The Theil-Sens' slope was then calculated to get the rate of change (Theil, 1950; Sen, 1968). Mean annual maximum, average, and minimum temperature values were computed from daily data, and years with more than 15 missing values were eliminated (Venable et al., 2012). Using the filled original SNOTEL temperature data, trends were computed for the entire time series, for the data before the sensor change, and for the data after the sensor change

(Table 1). Trends were also computed for the entire period of record and pre-sensor change period for the three adjusted datasets.

2.6 Snow Water Equivalent Modeling

To evaluate the three-homogenization methods, a simple temperature-based daily SWE model was applied to determine which of the homogenization algorithm performed the best. This model only uses observations of temperature (T) in degrees Celsius, precipitation (P) in millimeters, and two parameters (Kampf and Richer, 2014), as follows:

$$SWE_i = SWE_{i-1} - \alpha T_i \quad \text{if } T_i > T_s$$
$$SWE_i = SWE_i + P_{snow-i} \quad \text{if } T_i \leq T_s \quad \text{(Equation 2)}$$

where α is the melt coefficient parameter in mm/day/degree C, T_s is the threshold temperature parameter separating rain and snow, and i indicates day.

SWE was modeled for each year at each SNOTEL station using the original, H1, H2 and H3 average pre-sensor change temperature datasets. Two model parameters, T_s and α, were calibrated using the post-sensor change period of record (~2006 to 2015). Three different statistical-evaluation periods were assessed in daily SWE modeling: all days, snow months only (October through June), and melt months only (March through May) because it is more representative to use the snowmelt season with more snow cover on the ground than the entire accumulation and melt period during a year (Martinec et al., 2008; Guan et al., 2013). The Nash–Sutcliffe Coefficient of Efficiency (NSCE) and Bias were computed to evaluate the performance of the simulations. The Nash–Sutcliffe Coefficient of Efficiency calculated as:

$$NSCE = 1 - \frac{\sum_{i=1}^{n}(SWE_{obs} - SWE_{sim})^2}{\sum_{i=1}^{n}(SWE_{obs} - \overline{SWE})^2} \quad \text{(Equation 3)}$$

Where n is the total number of time steps, i is the time step, SWE_{obs} is the observed SWE and SWE_{sim} is the simulated SWE calculated from Equation 2. Values of NSCE can vary from 1.00

to -∞. An efficiency with a value of 1.00 indicates that simulation matches the observations, while an efficiency of lower than 0 indicates that the observed mean is better as a predictor than the model (Moriasi et al., 2007). Bias is used to measure the average tendency of the simulated data to be larger or smaller than their observed counterparts (Gupta et al., 1999). Bias is computed as follows:

$$\text{Bias} = \frac{(\sum_{i=1}^{n} SWE_{obs} - \sum_{i=1}^{n} SWE_{sim})}{\sum_{i=1}^{n} SWE_{obs}} \qquad \text{(Equation 4)}$$

Bias values with smaller absolute magnitude indicate better model simulation, and 0.0 is the optimal value (Gupta et al., 1999). Positive values indicate a model bias towards underestimation, while negative values indicate a model bias towards overestimation (Gupta et al., 1999). NSCE and bias values are considered "good" if $0.65 < \text{NSCE} \leq 0.75$ and $\pm 0.10 \leq \text{Bias} < \pm 0.15$. Models are considered "very good" if $0.75 < \text{NSCE} \leq 1.00$ and $\text{Bias} < \pm 0.10$ (Table 3). These criteria are stricter than the "satisfactory" rating for most model assessments because parameters are optimized during calibration but not during model evaluation (Moriasi et al., 2007). Parameters T_s and α over the post-sensor change period were optimized manually based on the values of NSCE and bias. The best-fit T_s and α were then applied to simulate SWE using the original and three homogenized temperature datasets over the pre-sensor change period. The starting date for each SNOTEL stations during the pre-sensor change period is the date of the first temperature measurement. Due to missing dates in GHCN-D system, years with more than 15 missing data were eliminated (Venable et al., 2012) in SWE modeling for H3.

Table 1. Temperature datasets and time periods used in the a) trend analysis, and b) calibration and evaluation of the SWE modeling.

Dataset	a) Trend analysis time period		b) SWE modeling
	Start	End	
Original entire	1980s	2015	N/A
Original pre-sensor change	1980s	1998 to 2006	evaluation
Original post-sensor change	1998 to 2006	2015	calibration
H1: Morrisey concurrent data	1980s	2015	evaluation (pre change only)
H2: Oyler adjustment	1980s	2015	evaluation (pre change only)
H3: GHCN adjacent station(s)	1980s	2015	evaluation (pre change only)

Table 2. Information for the four SNOTEL stations with paired GHCN-D stations used for H3

SNOTEL stations	Latitude	Longitude	Elevation (m)	Paired GHCN-D stations	Latitude	Longitude	Elevation (m)
Bison				Glenwood			
Lake	39.76487	-107.357	3316	Spgs #2	39.53964	-107.321	1775
Crosho	40.16745	-107.057	2774	Yampa	40.15327	-106.905	2403
Fremont							
Pass	39.37991	-106.197	3475	Climax	39.36859	-106.187	3451
				Aspen #1			
				SW	39.18542	-106.835	2488
Kiln				Leadville			
				Lake CO			
	39.31724	-106.615	2926	Airport	39.23095	-106.317	3029

Table 3. Performance ratings for hydrologic models based on the Nash-Sutcliffe Coefficient of Efficiency (NSCE) and Bias (Moriasi et al., 2007).

Performance Rating	NSCE	Bias
Very good	$0.75 < NSCE \leq 1.00$	$Bias < \pm 0.1$
Good	$0.65 < NSCE \leq 0.75$	$\pm 0.1 \leq Bias < \pm 0.15$
Satisfactory	$0.50 < NSCE \leq 0.65$	$\pm 0.15 \leq Bias < \pm 0.25$
Unsatisfactory	$NSCE \leq 0.50$	$Bias \geq \pm 0.25$

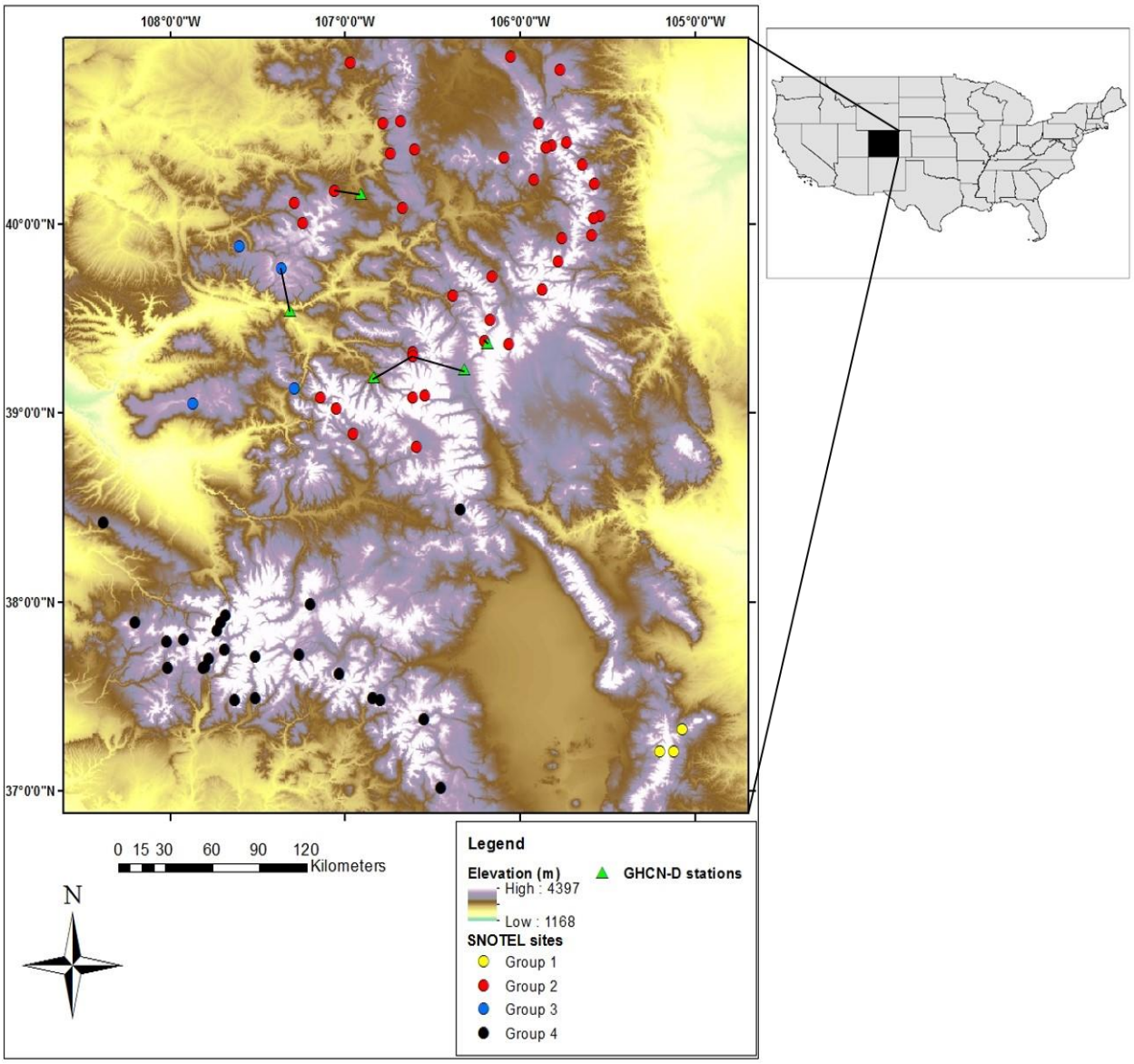

Figure 2. Map of the 68 long-term SNOTEL study stations, some shown with their paired GHCN-D stations (connected by black lines). SNOTEL stations are divided into four groups based on their precipitation variability (Wolter, 2001).

CHAPTER 3: RESULTS

3.1 Trend Analysis

From the filled original dataset over 1980s to 2015, a majority of the trends were warming annual temperatures (Table 2). This was especially true for the average and minimum temperatures where 99% of all SNOTEL study stations (expect Arrow) were warming significantly ($\alpha \leq 0.1$ level of significance). Additionally, 99% of these stations with a statistically significant trend for minimum temperature were at $\alpha = 0.001$ level of significance. More of the maximum temperatures were warming (54% of all study stations) than cooling (26% of all study stations), but fewer trends were significant. For the pre-sensor change period 1980s - 2006, most of the stations were experiencing significant warming trends for maximum (76% of all study stations), average (82% of all study stations) and minimum (85% of all study stations) temperature datasets. However, much fewer were warming significantly for all three datasets during the post-change period (Table 4).

When the H1 correction was applied, fewer stations were significantly warming, and the average rate of warming was at a lower rate over 1980 to 2015. From the filled original dataset, the greatest computed warming rates were 2.1 and 2.0 C° per decade for maximum and minimum temperatures, respectively; these rates were reduced to 1.6 and 1.2 C° per decade for the adjusted H1 datasets. Similarly, trends with H2 indicated the greatest warming was 1.9 C° per decade for maximum temperature and 1.2 C° per decade for minimum temperature. Overall, although all trends computed from three different datasets are generally warming, the trends tend to be smaller with two adjusted datasets compared to the original dataset (Table 4, Figure 3a, 3c). Ratios between trends from the original datasets and H1 datasets for maximum, average, and

minimum temperature were all below the 1 to 1 line (Figure 3a), indicating that the original datasets had greater trends than H1 datasets (Table 4, Figure 3a). Figure 3c illustrates that ratios between the original and H2 datasets for a majority of the average and all minimum temperature were below 1 to 1 line, with mainly positive values. This figure emphasizes that the original datasets had greater trends than H2 dataset as well, but in average and minimum temperature only. In addition, most of the trends for maximum, average, and minimum temperature for both original and H2 were positive. Figure 3b, 3d and 3e are quantile box plots showing the medians and ranges of +/- one standard deviations for H1 (Morrisey), H2 (Oyler), and Original temperature datasets.

Figure 4 illustrates an example of different magnitudes of trends in minimum temperature derived from pre-sensor change, post-sensor change data, original, H1 and H2 for Spud Mountain SNOTEL station. The original annual average minimum temperature had a step-like shift between 2004 and 2005, which was when temperature sensors were upgraded for Spud Mountain SNOTEL station. The original annual average minimum temperature shows a significant positive trend of 1.1°C per decade from 1987 to 2015 (Figure 4). Pre-sensor change data also demonstrated a significant positive trend but much smaller magnitude of 0.5°C per decade, while post-sensor change data showed the same warming rate but not statistically significant (Figure 4). Results from both H1 and H2 indicated much smaller trends of 0.4 and 0.3°C per decade compared to the original dataset over the entire time period (Figure 4).

For H3, Table 7 shows that average trends of maximum, average, and minimum temperature calculated from H3 were much smaller and less significant (expect Kiln) compared to the original datasets. Trends lowered from 0.1 °C per decade (maximum temperature from

Bison Lake) to 2.5 °C per decade (minimum temperature from Fremont Pass). Results from Kiln indicated higher and more significant trends in H3 compared to the original dataset.

3.2 SWE Modeling

SWE simulations were calibrated to observed SWE using the post-sensor change data, and then evaluated using other three temperature datasets. To evaluate the performances of three homogenization methods in the SWE modeling, we compared NSCE and bias values derived from daily SWE modeling for all days, snow months only (October through June), and melt months only (March through May) from all SNOTEL study stations using the original, H1, H2 and H3 average pre-sensor change temperature datasets.

3.2.1 Calibration

The calibrated values of T_s for the SWE simulations ranged from 0.4 to 7.2 °C with an average value of 4.1 °C, and calibrated values of α range from 0.6 to 4.9 mm/d/°C with an average value of 2.9 mm/d/°C. The calibration parameters T_s and α varied depending on the SWE data used and the statistical-evaluation periods used for performance statistics: all days, snow months only, or melt months only (Figure 5). Figure 6, 7, Table 6a, 6b and 6c illustrate the performance of the calibration (post-sensor change) daily SWE simulation. Figure 6a and 7a show that for evaluations of simulations over all days, 97% of the study stations were at "very good" model performance rating with values of NSCE greater than 0.75 and values of bias less than 0.1(Figure 6a, Figure 7a, Table 6a). For snow months only and melt months only, 96% and 84% of the study stations had "very good" model performance (Figure 6b, 6c, Figure 7b, 7c, Table 4b, 4c).

3.2.2. SWE Model Performance Using the Original, H1 and H2 Temperatures

The simulations using the original dataset during the pre-sensor change time period for all days had NSCE values ranging from -1.19 to 0.95 with a mean value of 0.73 (Figure 6a), and bias ranging from -1.22 to 0.18 with a mean value of -0.24 (Figure 7a), indicating a tendency for the simulations to over-estimate SWE values. Results showed 30% of the study stations were within "good" and "very good" performing ratings for all days. SWE model performance using the H1 dataset indicated that 84% of the study stations were considered as "good" and "very good" during all days statistical-evaluation period (Table 6a). Values of NSCE for H1 ranged from 0.06 to 0.97 with an average of 0.87 (Figure 6a), and values of bias ranged from -0.56 to 0.16 with an average of -0.08 (Figure 7a). For H2, 69% of the study stations were within the range of "good" and "very good" performing ratings during all days statistical-evaluation period (Table 6a). NSCE values varied from -1.48 to 0.97 with mean value of 0.81, and bias values varied from -1.18to 0.57 with mean of 0.07 (Figure 6a, 7a). NSCE values of both H1 and H2 improved by an average of 0.14 and 0.08, while bias values increased by an average of 0.16 for H1 and 0.31 for H2 compared to the original dataset.

Performance metrics for snow months only (October through June) illustrated that 29%, 84% and 62% of the study stations from the original, H1 and H2 were within "good" and "very good" performance ratings (Table 6b). Mean NSCE values were 0.67, 0.84 and 0.59 while mean bias values were -0.24, -0.07 and 0.10 for the original, H1 and H2, respectively. NSCE values from H1 dataset illustrated an average improvement of 0.17, but the mean NSCE values from H2 dataset lowered by 0.08 compared to the original dataset correspondingly for snow months only (October through June). Bias values from H1 and H2 datasets showed average improvements of 0.17 and 0.34 compared to the original dataset for this statistical-evaluation period.

For the melt months only (March through May), results indicated that 23%, 69% and 44% of the study stations had "good" and "very good" performance ratings for original, H1, and H2 temperature datasets (Table 4c). Values of NSCE varied dramatically for this period and ranged from -11.23 to 0.90 for the original dataset, -0.31 to 0.94 for H1 dataset and -3.45 to 0.89 for H2 dataset (Figure 6c). Bias values also varied from -1.93 to 0.15, -0.66 to 0.23, and -0.66 to 0.74 for the original, H1 and H2 datasets (Figure 7c). Results of NSCE derived from H1 showed an average improvement of 0.43 compared to the original dataset, and H2 indicated an average improvement of 0.20 compared to the original dataset. Bias values from H1 and H2 demonstrated average increases of 0.19 and 0.36, respectively. All average NSCE values of H1 and H2 for all three statistical-evaluation periods improved compared to the original dataset, and bias values for H1 and H2 were closer to 0.0 (optimal) as well.

Overall, the homogenized temperature values in H1 and H2 improved the performance of SWE simulation compared to the original temperature values, with H1 performing better than H2. However, the relative performance of the three temperature scenarios varied between stations. Figure 8a illustrates an example in which the original dataset had the best performance for SWE modeling. From this figure, simulated SWE using the original temperature dataset had a "very good" performance rating with 0.95 for NSCE and 0.03 for bias. The simulations for all three temperature datasets tended to under-estimate the SWE for both snow years, but the simulation with the original temperature dataset was closest to the observed SWE. Figure 8b shows an example of SWE modeling in which H1 yielded the best results among all three datasets, within "very good" performance rating of NSCE=0.95 and bias=0.00. The simulations for both original and H1 tended to over-estimate the peak SWE, whereas the simulation for H2 tended to under-estimate the peak. Figure 8c is an example in which H2 had the best modeling

performance among all datasets with NSCE value of 0.97 and bias value of 0.02. SWE simulation using H2 in this case had the most similar shape to the observed SWE, while the other two datasets tend to over-estimate the peak SWE.

3.2.3 SWE model performance using H3 temperature

SWE modeling for H3 was separated from other two datasets because of the limited study stations and the elimination of the years. Total eliminated years ranged from 15% (Crosho) to 59% (Fremont Pass) of the pre-sensor change period. Table 7 demonstrates the results of the H3 performance. Average NSCE improvements (compared to the original temperature dataset) for the four selected SNOTEL stations during all days were 0.09, 0.07 and 0.11 for H1, H2 and H3 datasets respectively. Values of bias for H1, H2 and H3 during all days also increased compared to the original dataset by an average of 0.13, 0.22 and 0.23 (Table 7), indicating better model performance in this case since the absolute magnitudes of the bias of all three homogenized temperature datasets are much smaller compare to the original temperature dataset.

Table 4. Average [and percent of all 68 SNOTEL study stations in brackets] of trends in degrees Celsius per decade for annual maximum, average, and minimum temperatures for the original, H1 and H2 datasets with significant and non-significant increasing and decreasing trends from 1980s to 2015. Trends are considered significant if $\alpha \leq 0.1$.

	entire period of record (1980s-2015)	maximum		average		minimum	
Dataset	Direction	signif. [% of stations]	non signif.	signif.	non signif.	signif.	non signif.
	Increasing +	0.65 [54]	0.17 [26]	0.95 [99]	0.24 [1]	1.22 [99]	0.18 [1]
Original	Decreasing -	0.60 [7]	0.11 [12]	N/A [0]	N/A [0]	N/A [0]	N/A [0]
	Total	0.50 [62]	0.082 [38]	0.95 [99]	0.24 [1]	1.22 [99]	0.18 [1]
H1 (Morrisey adjustment)	Increasing +	0.59 [28]	0.15 [25]	0.44 [79]	0.13 [19]	0.53 [91]	0.19 [6]
	Decreasing -	0.06 [16]	0.13 [31]	N/A [0]	0.23 [2]	N/A [0]	0.24 [3]
	Total	0.16 [44]	0.01 [56]	0.44 [79]	0.10 [21]	0.53 [91]	0.04 [9]
H2 (Oyler's adjustment)	Increasing +	0.58 [93]	0.27 [4]	0.54 [96]	0.17 [3]	0.51 [87]	0.10 [13]
	Decreasing -	0.06 [1]	0.07 [2]	N/A [0]	0.13 [1]	N/A [0]	N/A [0]
	Total	0.57 [94]	0.19 [6]	0.54 [96]	0.07 [4]	0.51 [87]	0.10 [13]
	pre-sensor change (1980s-2006)	maximum		average		minimum	
Dataset	Direction	signif.	non signif.	signif.	non signif.	signif.	non signif.
	Increasing +	1.05 [76]	0.32 [13]	0.77 [82]	0.30 [13]	0.78 [85]	0.39 [12]
Original	Decreasing -	N/A [0]	0.52 [11]	0.18 [2]	0.18 [3]	N/A [0]	1.08 [3]
	Total	1.05 [76]	0.05 [24]	0.72 [84]	0.21 [16]	0.78 [85]	0.09 [15]
H1 (Morrisey adjustment)	Increasing +	0.88 [72]	0.53 [13]	0.61 [81]	0.20 [12]	0.67 [78]	0.34 [18]
	Decreasing -	0.11 [6]	0.18 [9]	0.21 [1]	0.20 [6]	0.17 [1]	0.11 [3]
	Total	0.73 [78]	0.25 [22]	0.56 [82]	0.07 [18]	0.63 [79]	0.27 [21]
H2 (Oyler's adjustments)	Increasing +	0.98 [93]	0.22 [4]	0.94 [91]	0.36 [7]	0.93 [82]	0.48 [16]
	Decreasing -	N/A [0]	0.29 [3]	N/A [0]	0.87 [2]	N/A [0]	1.25 [2]
	Total	0.98 [93]	0.02 [7]	0.94 [91]	0.15 [9]	0.93 [82]	0.34 [18]
	post change (2000s-2015)	maximum		average		minimum	
Dataset	Direction	signif.	non signif.	signif.	non signif.	signif.	non signif.
Original	Increasing +	1.50 [9]	0.70 [65]	0.99 [13]	0.66 [84]	1.43 [21]	0.84 [73]
	Decreasing	0.26 [1]	0.40 [25]	N/A [0]	0.10 [3]	N/A [0]	0.30 [6]
	Total	0.91 [10]	0.39 [90]	0.99 [13]	0.63 [87]	1.43 [21]	0.75 [79]

Table 5. Average trends in degree Celsius per decade for annual maximum, average, and minimum temperature for the original and H3. (If the trend is significant, level of significance listed in brackets: ***: α=0.001 level of significance; **: α=0.01 level of significance; *: if α=0.05 level of significance; +: if α=0.1 level of significance)

	maximum		average		minimum	
Stations	Ori	H3	Ori	H3	Ori	H3
Bison Lake	0.4 [*]	0.3	0.5[**]	0.2	0.7 [*]	0.8 [+]
Crosho	1.1 [***]	0.1	0.9 [***]	0.2	1.1 [***]	0.3 [*]
Fremont Pass	1.5 [***]	0.2	1.3 [***]	-0.5	1.1 [***]	-1.4 [*]
Kiln	0.8 [**]	0.9 [***]	0.5 [**]	0.8 [***]	0.6 [**]	0.6 [**]

Table 6. Numbers [and percent count in brackets] of the study stations that are within different performance ratings (Moriasi et al., 2007) from SWE modeling performance using daily data, (a) all days (total 68 stations for calibrated, original, H1 and H2; results of H3 is shown in Table 7), (b) snow months only (October through June), and (c) melt months only (March through May).

(a) All days	Calibrated (n=68)	Original (n=68)	H1 (n=68)	H2 (n=68)
Very Good	66[97]	10[15]	44[65]	34[50]
Good	1[1.5]	10[15]	13[19]	13[19]
Satisfactory	1[1.5]	22[32]	6[9]	12[18]
Unsatisfactory	0	26[38]	5[7]	9[13]

(b) October-June	Calibrated (n=68)	Original (n=68)	H1 (n=68)	H2 (n=68)
Very Good	65[96]	9[13]	44[65]	30[44]
Good	1[1]	11[16]	13[19]	12[18]
Satisfactory	2[3]	25[37]	6[9]	13[19]
Unsatisfactory	0	23[34]	5[7]	13[19]

(c) Mar-May	Calibrated (n=68)	Original (n=68)	H1 (n=68)	H2 (n=68)
Very Good	57[84]	9[13]	30[44]	19[28]
Good	6[9]	7[10]	17[25]	11[16]
Satisfactory	3[4]	17[25]	10[15]	17[25]
Unsatisfactory	2[3]	35[52]	11[16]	21[31]

Table 7. Comparison of NSCE and bias values from modeling SWE using original, H1, H2 and H3 datasets over years with complete temperature data (<15 years missing data)

	Original		H1		H2		H3	
Entire Year	NSCE	Bias	NSCE	Bias	NSCE	Bias	NSCE	Bias
Kiln	0.92	-0.12	0.96	0.04	0.93	0.10	0.91	0.14
Fremont Pass	0.70	-0.25	0.84	-0.13	0.89	0.11	0.90	0.04
Crosho	0.60	-0.39	0.83	-0.21	0.82	-0.21	0.92	-0.08
Bison Lake	0.86	0.16	0.81	0.22	0.73	0.29	0.80	0.21
Oct-Jun								
Kiln	0.89	-0.14	0.95	0.03	0.91	0.10	0.91	0.12
Fremont Pass	0.65	-0.19	0.79	-0.10	0.84	0.11	0.86	0.05
Crosho	0.51	-0.38	0.79	-0.21	0.78	-0.21	0.90	-0.08
Bison Lake	0.79	0.17	0.71	0.22	0.60	0.29	0.69	0.22
Mar-May								
Kiln	0.78	-0.17	0.92	0.05	0.85	0.13	0.84	0.14
Fremont Pass	-23.09	-0.97	-4.19	-0.42	0.75	0.05	0.55	0.06
Crosho	0.19	-0.47	0.68	-0.24	0.66	-0.23	0.86	-0.09
Bison Lake	0.40	0.18	-0.03	0.27	-0.21	0.30	-0.03	0.25

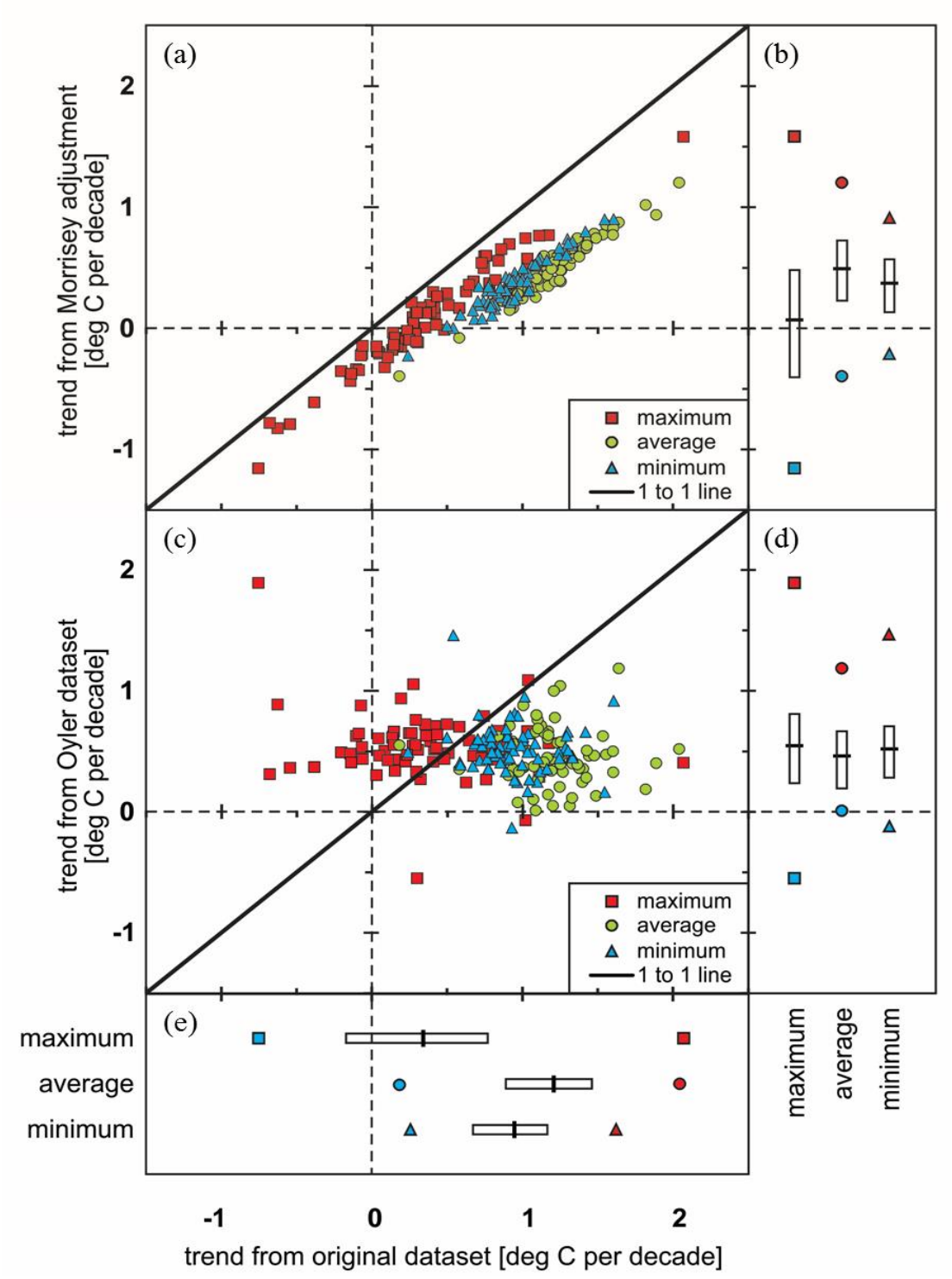

Figure 3. Comparison of temperature trends from the adjusted data using (a) H1 (Morrisey) and (c) H2 (Oyler) versus those computed from the original data over 1980s to 2015. Estimated sensor bias within one standard deviation for maximum, average and minimum temperature for (b) H1 (Morrisey), (d) H2 (Oyler), and (e) Original temperature datasets. Red refers to the maximum value, whereas the blue is the minimum value; Lines in the middle of the hollow boxes are the medians, and the bars are quantile box plots.

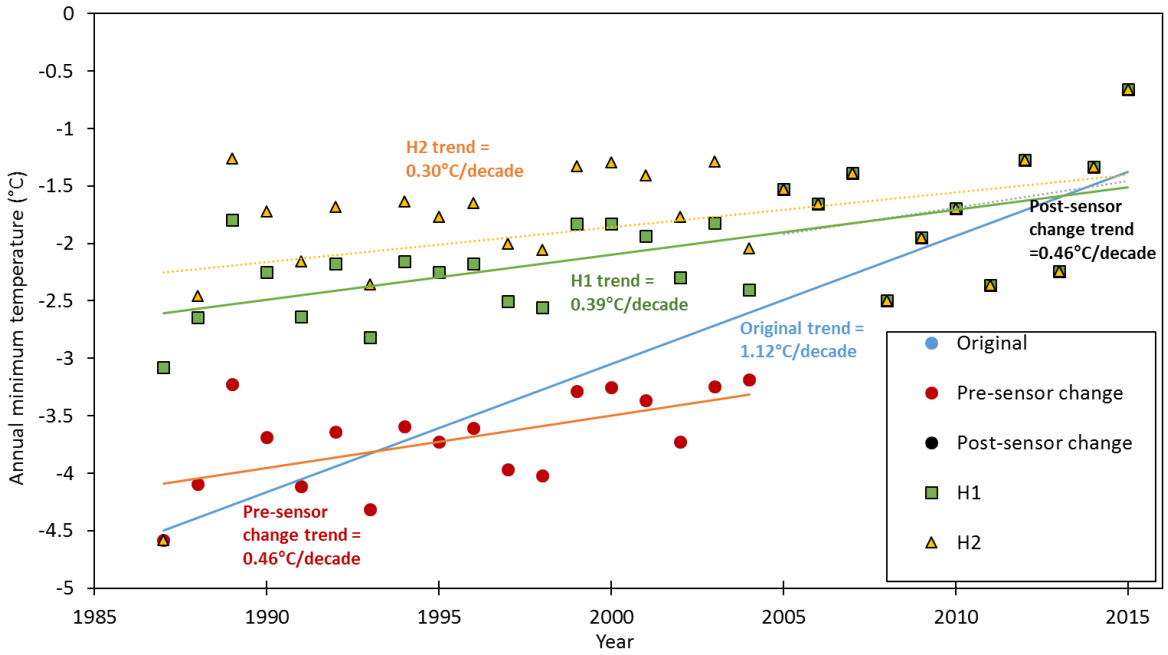

Figure 4. Plot of mean annual minimum temperature (°C) for the Spud Mountain SNOTEL station. Trend lines were fit to the data according to the different time periods. Dotted lines represent no statistical significance.

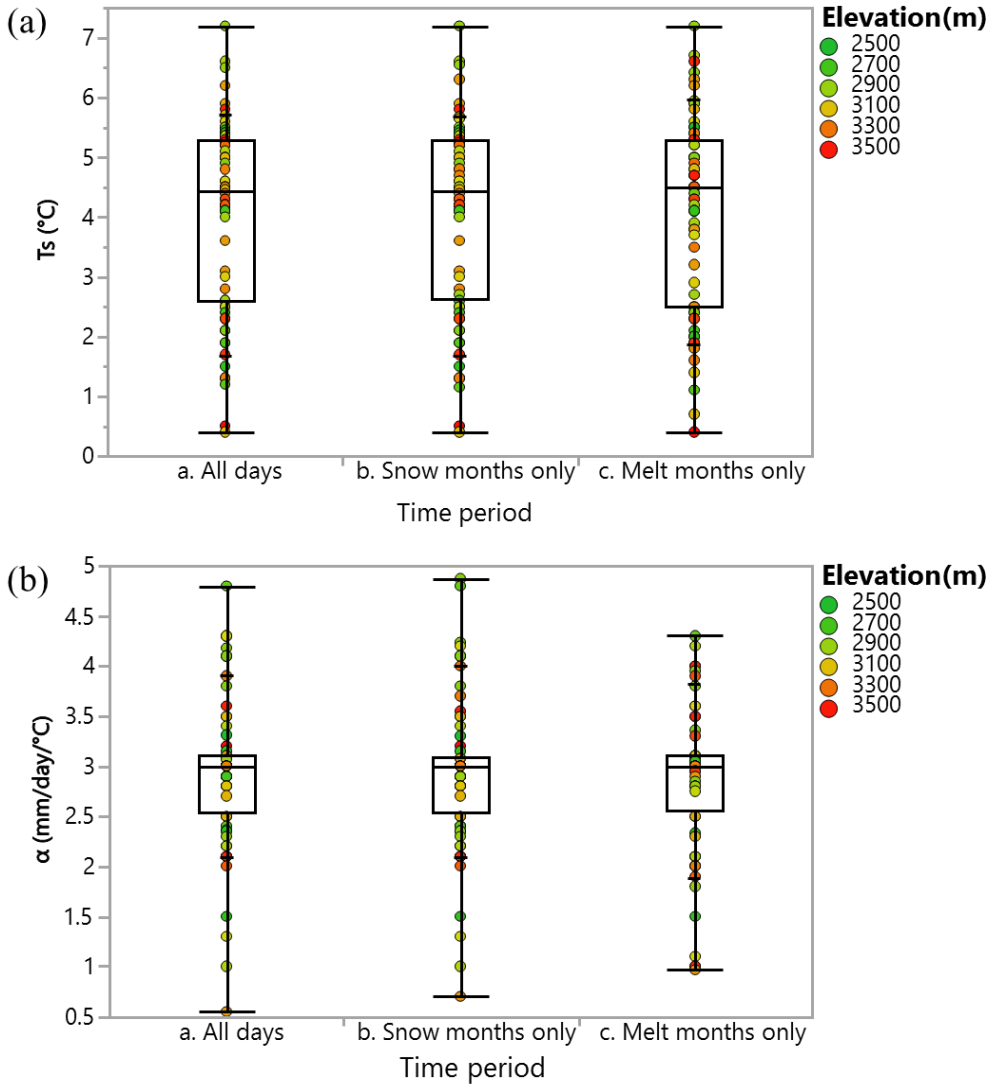

Figure 5. Range of values of the calibration parameters (a) T_s and (b) α, for all days, snow months only (October through June), and melt months only (March through May). Both plots (a) and (b) are quantile box plots, and the whiskers on plot correspond to the quantiles in the distribution output (top horizontal line: 100%, top line of the box: 75%, middle line in the box:50%; bottom line of the box: 25%; botton line: 0%).

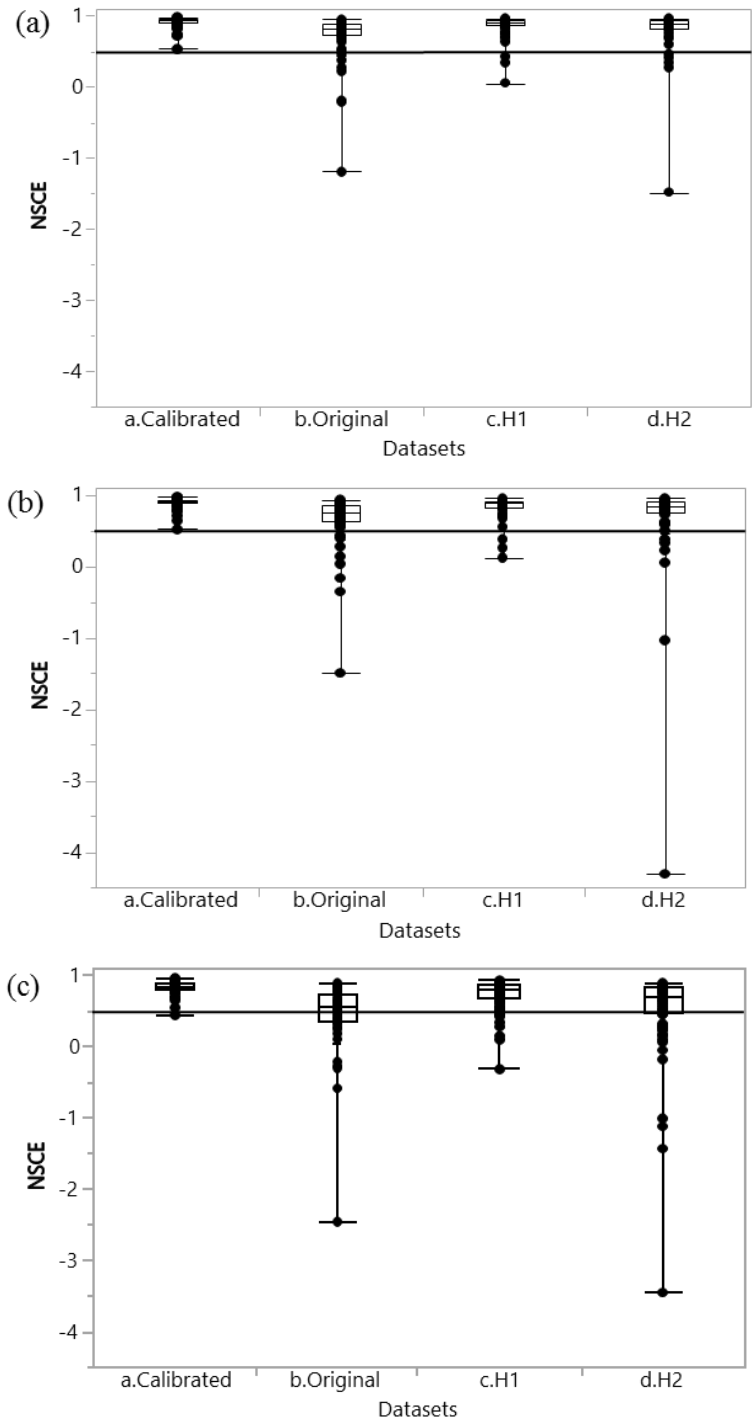

Figure 6. Comparison of NSCE values from the SWE simulations using calibrated (over post-sensor change period), original, H1 and H2 temperature datasets (over pre-sensor change period) for (a) all days, (b) snow months only (October through June) and (c) melt months only (March through May). (Plots are quantile box plots; Two data points with NSCE= -6.07 from H2 and NSCE= -11.23 from the original data were removed from plots (b) and (c) for figure consistency, solid line = 0.5 is the model satisfactory performance rating)

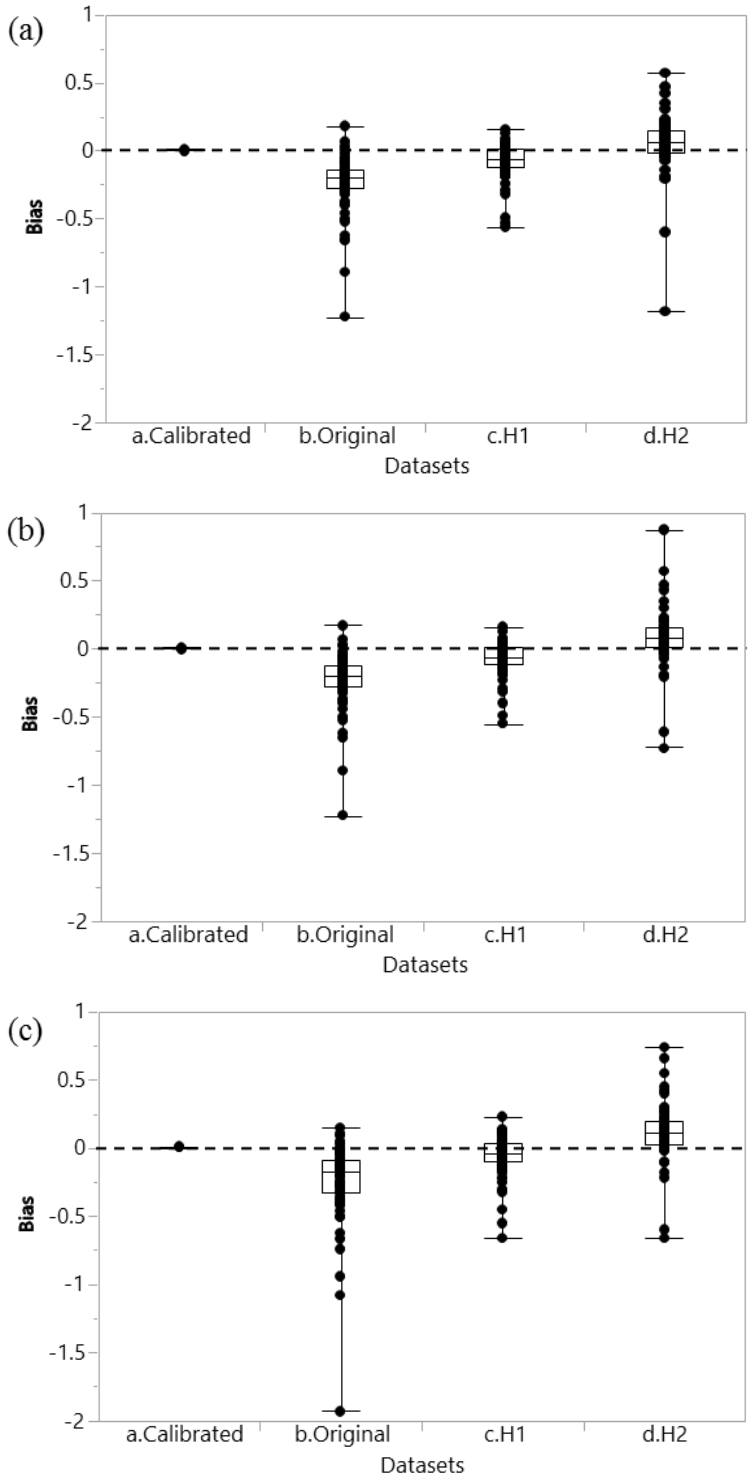

Figure 7. Comparison of bias values from the SWE simulation using calibrated (over post-sensor change period), original, H1 and H2 datasets (over pre-sensor change period) for (a) all days, (b) snow months only (October through June), and (c) melt month only (March through May). (Plots are quantile box plots, dotted line = 0 is the optimal value of bias)

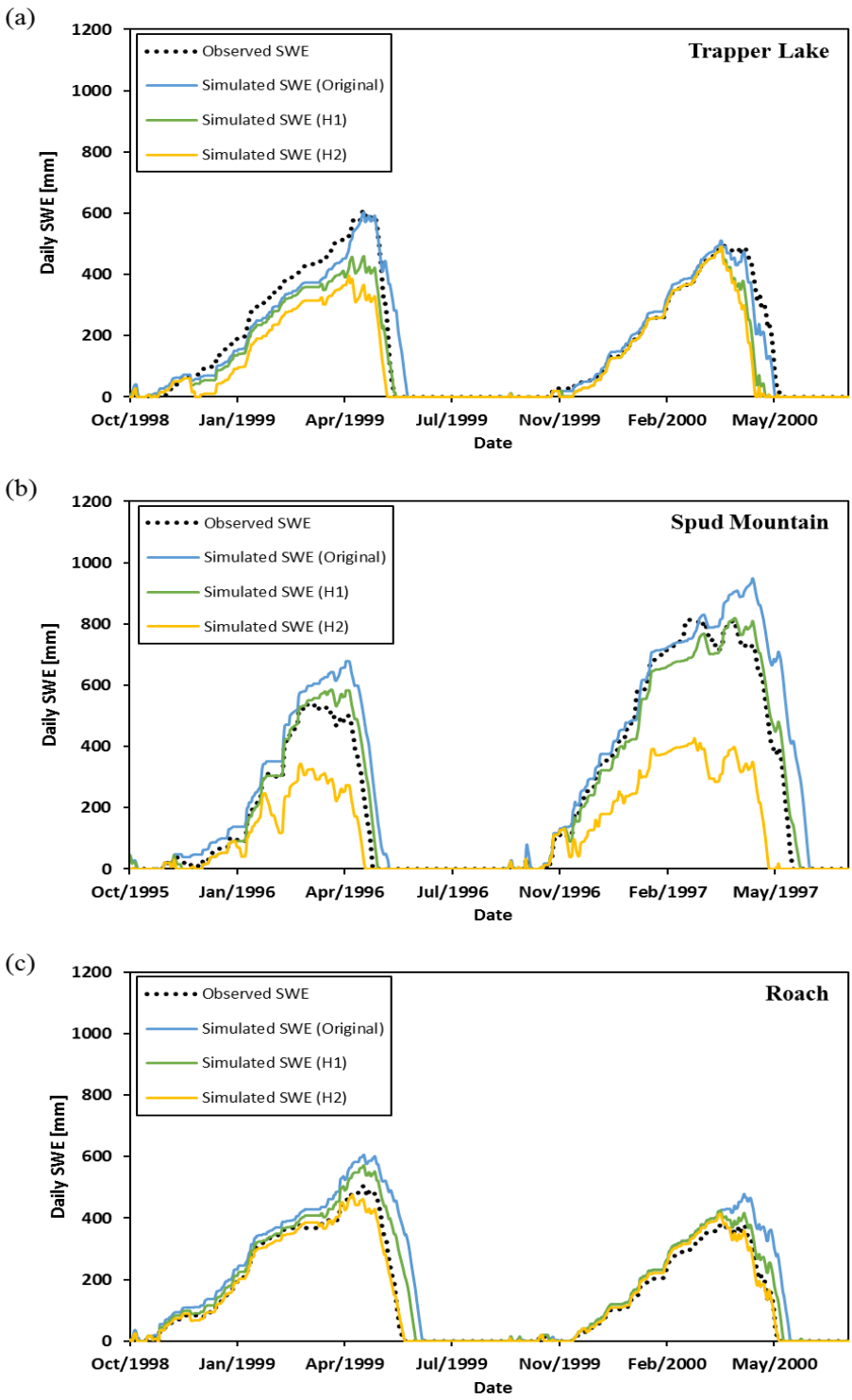

Figure 8. Example observed and simulated SWE for sequential years using the original, H1, and H2 temperature values for the (a) Trapper Lake SNOTEL station for 1999 (low) and 2000 (high), (b) Spud Mountain SNOTEL station for 1996 (low) and 1997 (high), and (c) Roach SNOTEL station for 1999 (high) and 2000 (low).

CHAPTER 4. DISCUSSION

4.1. Warming in the Southern Rocky Mountains of Colorado

Similar to previous studies (Clow, 2010; Pederson et al., 2011; Harpold et al., 2012; Rangwala and Miller, 2012), we found a significant trend of 0.95 °C per decade using the original average temperature data from 68 long term SNOTEL study stations across Colorado for the period from the 1980s to 2015. This trend is much greater than the trends at lower elevations (Hansen et al., 2010; Oyler et al., 2015). The majority of the stations (>82%) show significant positive trends in both average and minimum temperature for the entire time of records and pre-sensor change period, while only a few stations show significant trends for the post-sensor change time period (Table 4). Maximum temperature for both the entire time and pre-sensor change period shows less significant and smaller positive trends compared to average and minimum temperature datasets (Table 4), which is consistent with the findings from Oyler et al. (2015).

Snow-albedo feedback, which increases the absorption of solar radiation due to the decreasing in snow cover and therefore albedo, was introduced as a main cause for elevation-dependent warming in southern and northern Rocky Mountains (Clow, 2010; Pederson et al., 2011). However, as discussed in Rangwala and Miller. (2012), snow-albedo feedback leads to greater warming rates for maximum temperature since solar radiation absorption increases during daytime. Hence, although the temperature trends from the SNOTEL network are distinctly different from the trends of lower elevations, the relatively small trends in maximum temperature suggest that snow-albedo feedback was not the cause of high and low elevation differences. Additionally, step-like shifts in temperature datasets especially minimum

temperature were found in SNOTEL temperature records (e.g. Figure 4), which is again consistent with the findings from Oyler et al. (2015) and Rangwala et al. (2015). An artificial rise or drop in temperature, which results from changes in locations or sensor exposure, tends to have a more definite effect on minimum temperature than maximum temperature. The minimum temperature usually occurs at the time of sunrise with calm and steady boundary conditions when surface temperature is heavily coupled to the characteristics of the immediate surroundings. During the daylight, the boundary layer is generally well mixed, thus the differences of microclimates between the pre and post sensor locations is less evident for maximum temperatures (Menne et al., 2009). Both the step-like temperature shifts and the larger trends in minimum temperature indicate that the temperature sensor changes in the SNOTEL network magnified the warming at higher elevations, which delivered an "artificial amplified" (Oyler et al., 2015) elevation dependent warming signal across Colorado. Users of temperature data provided by the SNOTEL network should be careful when choosing the time periods to analyze, especially for trend investigations.

4.1.1 Warming Trends with Homogenized Datasets

Results from Table 4 demonstrate that both H1 and H2 yielded lower rates of change for minimum [(average of 0.69 and 0.71 °C per decade for H1 and H2)], average [(average of 0.51 and 0.41 °C per decade for H1 and H2)] and maximum [(average of 0.06 and 0.07 °C per decade for H1 and H2)] temperature, compared to the original datasets. However, a majority of the SNOTEL stations (>79%) still show significant warming in both minimum and average temperature. Therefore, even with the inhomogeneities in the historical temperature observations in SNOTEL network across Colorado caused by temperature sensor change, warming at higher elevations is still significantly greater than lower elevations and should not be neglected. Others

have found evidence of elevation dependent warming in Colorado and other parts of the western United States (Diaz and Eischeid, 2007), but we did not notice any apparent correlation between elevations and warming rates in our study. Identifying the patterns and mechanisms of elevation dependent warming is difficult because of sparse long-term meteorological stations at high elevations (Pepin et al., 2015) and spatial and temporal variability, which is even seen within terrain considered homogeneous (Pielke et al., 2002; Rangwala and Miller, 2012; Fassnacht et al., 2016).

4.2. Homogenization Methods

The NSCE and bias statistics derived for SWE modeling illustrate that both H1 and H2 datasets have improved the performance of the SWE simulation compared to the original datasets for both NSCE and bias. As shown in Tables 6a-c, NSCE and bias values from SWE modeling using H1 indicate 84%, 84% and 69% of the study stations are within the "good" and "very good" performance rating for all days, snow months only, and melt months only, respectively. Likewise, H2 yields "good" and "very good" results at many stations with 69% for all days, 62% for snow months only, and 44% for melt months only (Tables 6a-c). H1 homogenized data lead to dramatic improvements compared to the original data for which >23% of the study stations had "good" or "very good" performance ratings. H2 also improves modeling performance compared to the original data, but it does not improve as much as H1. Hence, H1 is the better homogenization method according to the SWE model performance. Additionally, trends from H1 datasets shown in the histogram (Appendix Figure A-1) have a range of variability that is similar to the original temperature datasets, whereas H2 datasets tend to over-smooth the trends (e.g. Figure 1a). The H1 homogenization method may perform better than H2 probably is because it is computed from comparing old and new temperature sensors with the

same configuration in the relative same locations in Idaho, and the adjustments vary with temperature. On the other hand, the H2 adjustments are derived using the USHCN stations, which are at lower elevations than SNOTEL stations. The USHCN stations may not fully represent the SNOTEL station temperature variability, since each station has a distinct climatic condition and location. Previous studies have shown that there could be large differences in temperature even in much more homogenous terrains (Pielke et al., 2002; Fassnacht et al., 2016), while mountain regions have more pronounced spatial variability (Rangwala and Miller, 2012; Patterson, 2016). H2 adjustments are also fixed to remain the same with low and high temperatures, and this likely accounts for the more limited ranges of temperature trends after homogenization. H3 is also derived from lower elevation GHCN-D stations, similar to Oyler et al. (2015), but the adjustments are temperature-dependent as the H3 temperature is a function of the original temperature. The intent of the H3 analysis is not to redo the effort of Oyler et al. (2015), so only four SNOTEL stations were paired with GHCN-D stations to illustrate site specific variability (Table 7). Evaluation of H3 temperature adjustments were limited by the missing data in GHCN-D stations, which reduced the range of years that could be tested.

H1 and H2 are applicable for many of the SNOTEL stations (>44%) in Colorado but not for all, possibly since not all temperature sensors were initially installed in the same location at the data collection hut, yet all were moved to the same location above the snow pillow. Temperature sensors were not part of the initial SNOTEL design so their addition, sometimes ten years after a SNOTEL station was established, was ad hoc. Previous research using *in situ* observations has noted the possibility of preferential cold air drainage at night near the hut, which would yield colder minimum temperatures during the pre-sensor change period compared to the current, common location above the snow pillow (Domonkos, 2016). From the SWE

simulation results, the median bias values for the original temperature data are all lower than 0.0 for the three statistical-evaluation periods (Figure 7a-c), suggesting that the original temperature records tended to be cold-biased (more simulated SWE than observed). However, differences in the range of cold bias between stations may have been caused by canopy changes at many stations caused by tree encroachment (e.g., Fassnacht and Hultstrand, 2015) or beetle kill of the trees. Due to safety reasons, some trees have been removed though the NRCS snow survey tried to diminish canopy changes particularly encroachment (Fassnacht and Ma, 2016). For example, Arrow station has been completely cleared of beetle killed trees by a private land owner around 2009 (Gillespie, 2012). Due to these types of changes, hemispherical canopy closure photographs should be to be taken on a regular basis at each SNOTEL station to monitor canopy changes. High resolution satellite imagery may also be available for the past decade to examine canopy changes at some SNOTEL stations (Fassnacht and Ma, 2016).

Although homogenized datasets produce more coherent trends (Figure 3) and improved SWE modeling results in most cases (Figure 8), performance of SWE simulations for the homogenized datasets is still a little worse than performance during the calibration time period (e.g. with an average NSCE lowered by 0.05 for H1 and by 0.11 for H2, while bias decreased by an average of 0.08 for H1 and increased by an average of 0.07 for H2 during all days). Therefore, it is essential to understand the limitations and uncertainties in the homogenization methods. Pielke et al. (2007) suggested that homogenization tends to neglect the uniqueness in climatic conditions from individual stations and over-smooth the trends (e.g. Figure 1a) because the homogenized data are integrated from the average temperatures of neighboring stations. This effect is similar to the use of the Regional Kendall Test (e.g., Clow, 2010) that produces a single trend among multiple stations, but has been shown to mask larger individual trends or even

trends in opposite direction (Fassnacht et al., 2016). Oyler et al. (2015) states that a standard homogenization procedure lacks the capability to account for strong seasonal dependencies, so it is not completely effective for solving the temperature inhomogeneities in the SNOTEL network. However, it is still informative to use homogenized data because it helps to interpret the patterns of climate variability and change at the surface (Menne et al., 2009). H3 shows similar or slightly worse performances compare to H2 (Table 7); therefore, a better site-specific method (with more complete temperature data, similar geographic and climatic conditions as the SNOTEL study stations) is recommended to replace H3 in the future.

4.3 SWE Modeling

Statistics from the calibrated SWE models show that the simple temperature-based model simulates SWE well (Tables 6a-c and Figure 8), with more than 85% of the study stations having "very good" performance ratings for the three statistical-evaluation periods (Tables 6a-c). Temperature based models perform well because air temperature plays an essential role in melting due to its link to longwave atmospheric radiation, which is an important heat source contributing to melt (Ohmura, 2001; Hock, 2003).

In the calibrated simulations, values of T_s ranged from 0.4 to 7.2 °C with similar distributions for all days, snow months only, and melt months only (Figure 5a). T_s values for calibrated stations with lower NSCE (<0.75) were all greater than 3.5 °C. Kampf and Richer (2014) also found that the model performs relatively well when T_s is within 0 to 3.3 °C. In reality, there is likely a difference between a T_s threshold that distinguishes rain from snow and a T_s for initiation of melt, but Kampf and Richer (2014) simplified the model by using one value for both to reduce the number of non-unique modeling solutions. The model can also be applied

with two separate temperature thresholds, one for snow fall versus rain fall (e.g., Fassnacht et al., 2013) and another for snow melt.

Melt factors also vary over time as a function of individual energy components that provide energy for melt, which depend on weather and surface type (Hock, 2003; Fassnacht et al., 2017). For this study, the melt factor α was assumed to be constant in time for each SNOTEL station to simplify the computation and calibration. The melt factor calibrated for the melt months only has a slightly smaller range of 1.0 to 4.3 mm/d/°C, compared to other two evaluation time periods (0.6 to 4.8 mm/d/°C for all days and 0.7 to 4.9 mm/d/°C for snow months only; Figure 4b). Values of the melt factor α are comparable to those identified in Kampf and Richer (2014) and Fassnacht et al. (2017).

No correlation (direct increasing or decreasing) has been found between the two model parameters and elevation (Figures 4a and b). Fassnacht et al. (2017) found that time explains about 70% of the variance in the computed snow melt factor across a similar domain, whereas elevation explains less than 10% of the remaining variance for stations not in evergreen forests. When examining smaller domains, such as watersheds, elevation can be more important in explaining the spatial variance in the snow melt factor (Fassnacht et al., 2017).

It is important for users to be aware of the limitations in modeling SWE while using temperature-based daily SWE model. A classical temperature-based method is only suitable for "average conditions" owing to spatial and temporal variability in energy balance components, which varies with weather and surface type (Hock, 2003). Likewise, input variables and parameters obatained from point measurements are often not representative at catchment scale because of the large small-scale variability in mountain terrian (Hock, 2003).

CHAPTER 5: CONCLUSIONS

This study evaluates the temperature products from long-term SNOTEL stations in Colorado over the period from the 1980s through 2015. These temperature products are all affected by a temperature sensor change. Results from trend analysis show a significant trend of 0.95 °C per decade using the original average temperature data from 68 long term SNOTEL stations in Colorado over their entire period of record. More than 82% of the study stations have significant positive trends in both average and minimum temperature for the entire period of record and pre-sensor change period, while only few stations show significant trends for the post-sensor change time period. Additionally, steplike shifts in temperature datasets especially minimum temperature were found in SNOTEL temperature records at the time of the temperature sensor change. The temperature sensor change in the SNOTEL network magnified the apparent warming at higher elevations.

Three homogenization methods were developed and tested using a simple temperature-based model to simulate SWE. Homogenization methods lowered the magnitude of temperature trends especially in minimum temperature (lowered to an average of 0.5 °C per decade). However, the majority of the SNOTEL stations (>79%) still showed significant warming in both minimum and average temperature. Hence, it is crucial to note that even with the inhomogeneities in the historical temperature observations in SNOTEL network across Colorado, these areas are still warming at a rate higher than the global average (Diaz and Eischeid, 2007).

SWE simulations with a temperature index model can test the performance of the temperature homogenization methods. Calibrated SWE models show an average NSCE of 0.88

and an average bias of 0.00 for all three statistical-evaluation periods: all days, snow months only (October through June), and melt months only (March through May). SWE models using the original pre-sensor change temperature data shows >23% of the stations are within "very good" and "good" performance model. Temperature homogenization improved SWE modeling performance, and >69% of the stations using H1 and >44% of the stations using H2 datasets are within "very good" and "good" performance ratings. NSCE generally improved for H1 and H2 compared to the original temperature data (0.25 and 0.07 for H1 and H2), whereas bias generally increased for H1 and H2 (0.18 and 0.34 for H1 and H2) to yield bias values closer to 0.0. Therefore, homogenization methods evaluated in this study are applicable for many of the SNOTEL stations in Colorado but not all, and need to be applied with caution in future climate change research.

Identifying the patterns and mechanisms of elevation dependent warming is difficult due to extremely sparse long-term meteorological stations at high elevations and the spatial and temporal variability of temperature in mountain terrain. Furthermore, accurate adjustment of the historical temperature dataset may not be possible. Therefore, high elevation mountian regions require more long-term climate monitoring stations to examine elevation-dependent warming in detail. We recommend that potential users of temperature products from the SNOTEL network be very careful about the time periods chosen for future climate change researchs and assessments. The H1 and H2 homogenizations evaluated in this study could be used to improve the continuity of the temperature records and correct the tempearture offset caused by sensor change in many cases, but not for all the SNOTEL stations across Colorado.

LITERATURE CITED

Ceppi, P., Scherrer, S. C., Fischer, A. M., and Appenzeller, C. (2010). Revisiting Swiss temperature trends 1959-2008. *International Journal of Climatology*, *32*(2), 203-213. doi:10.1002/joc.2260.

Colorado Water Conservation Board. (2015). Chapter 4. Water supply. *Colorado's water plan.* Retrieved from https://www.colorado.gov/pacific/cowaterplan/july-2015-second-draft-colorados-water-plan

Clow, D. W. (2010). Changes in the Timing of Snowmelt and Streamflow in Colorado: A Response to Recent Warming. *Journal of Climate, 23*(9), 2293-2306. doi:10.1175/2009jcli2951.1.

Diaz, H. F., and Eischeid, J. K. (2007). Disappearing "alpine tundra" Köppen climatic type in the western United States. *Geophys. Res. Lett, 34, L18707*. doi:10.1029/2007GL031253.

DeGaetano, A.T., Eggleston, K.L., and Knapp, W.W. (1995). A method to estimate daily maximum and minimum temperature observations. *Journal of Applied Meteorology,* 34, 371–380. doi:10.1175/1520-0450-34.2.371.

Domonkos, B. (2016). Personal communication. NRCS Colorado State Snow Survey Supervisor, Lakewood, CO.

Dosken, N., Climate -- Rocky Mountain High. *Colorado's Climate, The cocorahs 'state climate' series.* Retrieved from http://www.cocorahs.org/Media/docs/ClimateSum_CO.pdf

Doesken, N. J., Pielke, R. A., and Bliss, O. A. (2003, January). Climate of Colorado. Retrieved from http://climate.colostate.edu/climateofcolorado.php

Durre, I., Menne, M. J., Gleason, B. E., Houston, T. G., and Vose, R. S. (2010). Comprehensive Automated Quality Assurance of Daily Surface Observations. *Journal of Applied Meteorology and Climatology, 49*(8), 1615-1633. doi:10.1175/2010jamc2375.1

Eischeid, J. K., Pasteris, P. A., Diaz, H. F., Plantico, M. S., and Lott, N. J. (2000). Creating a Serially Complete, National Daily Time Series of Temperature and Precipitation for the Western United States. *Journal of Applied Meteorology, 39*(9), 1580-1591. doi:10.1175/1520-0450(2000)039<1580:cascnd>2.0.co;2

Fassnacht, S.R., Venable, N.B.H., Khishigbayar, J., and Cherry, M.L. (2013). The Probability of Precipitation as Snow Derived from Daily Air Temperature for High Elevation Areas of Colorado, United States. *Cold and Mountain Region Hydrological Systems Under Climate Change: Towards Improved Projections* (Proceedings of Symposium H02, IAHS-IAPSO-IASPEI Assembly, Gothenburg, Sweden, July 2013) IAHS, 360, 65-70

Fassnacht, S. R., and Records, R. M. (2015). Large snowmelt versus rainfall events in the mountains. *Journal of Geophysical Research: Atmospheres, 120*(6), 2375-2381. doi:10.1002/2014jd022753.

Fassnacht, S. R., Cherry, M. L., Venable, N. B., and Saavedra, F. (2016). Snow and albedo climate change impacts across the United States Northern Great Plains. *The Cryosphere, 10*(1), 329-339. doi:10.5194/tc-10-329-2016.

Fassnacht, S.R., López-Moreno, J.I., Ma, C., Pfohl, A.K.D., Kampf, S.K., and Kappas, M. (2017). Spatio-temporal Snowmelt Variability across the Headwaters of the Southern Rocky Mountains. *Front. Earth Sci., 11(3),* doi:10.1007/s11707-017-0641-4.

Guan, B., Molotch, N. P., Waliser, D. E., Jepsen, S. M., Painter, T. H., and Dozier, J. (2013). Snow water equivalent in the Sierra Nevada: Blending snow sensor observations with snowmelt model simulations. *Water Resources Research, 49*(8), 5029-5046. doi:10.1002/wrcr.20387

Gupta, H. V., Sorooshian, S., and Yapo, P. O. (1999). Status of Automatic Calibration for Hydrologic Models: Comparison with Multilevel Expert Calibration. *Journal of Hydrologic Engineering, 4*(2), 135-143. doi:10.1061/(asce)1084-0699(1999)4:2(135).

Harpold, A., Brooks, P., Rajagopal, S., Heidbuchel, I., Jardine, A., and Stielstra, C. (2012). Changes in snowpack accumulation and ablation in the intermountain west. *Water Resources Research, 48*(11), doi:10.1029/2012wr011949.

Hansen, J., Ruedy, R., Sato, M., and Lo, K. (2010). Global surface temperature change, *Rev. Geophys, 48*, RG4004, doi:10.1029/2010RG000345.

Hock, R. (2003). Temperature index melt modelling in mountain areas. *Journal of Hydrology, 282*(1-4), 104-115. doi:10.1016/s0022-1694(03)00257-.

Huth, R., and Nemešová, I. (1995). Estimation of Missing Daily Temperatures: Can a Weather Categorization Improve Its Accuracy? *Journal of Climate, 8*(7), 1901-1916. doi:10.1175/1520-0442(1995)008<1901:eomdtc>2.0.co;2.

IPCC, (2014). Topic 1: Observed Changes and their Causes. *Climate Change 2014: Synthesis Report. Contribution of Working Groups I, II and III to the Fifth Assessment Report of the Intergovernmental Panel on Climate Change [Core Writing Team, R.K. Pachauri and L.A. Meyer (eds.)]*. IPCC, Geneva, Switzerland, 151 pp.

Julander, R.P., Curtis, J., and Beard, A. (2007). The SNOTEL Temperature Dataset. *Mountain Views Newsletter, 1*(2), 4-7, http://www.fs.fed.us/psw/cirmount/.

Kampf, S. K., and Richer, E. E. (2013). Estimating source regions for snowmelt runoff in a Rocky Mountain basin: tests of a data-based conceptual modeling approach. *Hydrological Processes, 28*(4), 2237-2250. doi:10.1002/hyp.9751.

Kampf, S. K., and Lefsky, M. A. (2016). Transition of dominant peak flow source from snowmelt to rainfall along the Colorado Front Range: Historical patterns, trends, and lessons from the 2013 Colorado Front Range floods. *Water Resources Research, 52*(1), 407-422. doi:10.1002/2015wr017784.

Kampf, S. K. and Fassnacht, S. R. (2016). Snow. *Colorado Encyclopedia.* Retrieved from http://coloradoencyclopedia.org/article/snow

Kendall, M.G., and Gibbons, J.D. (1990). *Rank Correlation Methods (5th ed.)*. Hodder and Stoughton, London, UK.

Liu, X., Cheng, Z., Yan, L., and Yin, Z. (2009). Elevation dependency of recent and future minimum surface air temperature trends in the Tibetan Plateau and its surroundings. *Glob Planet Change*, 68, 164–174.

Mann, H. B. (1945). Nonparametric tests against trend. *Econometrica*, 13, 245-259.

Martinec, J., Rango, A., Roberts, R. (2008). *Snowmelt Runoff Model User's Manual*, Updated Edition 2008, WinSRM Version 1.11. New Mexico State University Agricultural Experiment Station, Special Report 100.

Mcguire, C. R., Nufio, C. R., Bowers, M. D., and Guralnick, R. P. (2012). Elevation-Dependent Temperature Trends in the Rocky Mountain Front Range: Changes over a 56- and 20-Year Record. *PLoS ONE, 7*(9). doi:10.1371/journal.pone.0044370.

Menne, M. J., Williams, C. N., and Vose, R. S. (2009). The U.S. Historical Climatology Network Monthly Temperature Data, Version 2. *Bulletin of the American Meteorological Society, 90*(7), 993-1007. doi:10.1175/2008bams2613.1.

Menne, M. J., and Williams, C. N. (2009). Homogenization of temperature series via pairwise comparisons, *J. Clim*, 22(7), 1700–1717. doi:10.1175/2008JCLI2263.1.

Moore, C., Kampf, S., Stone, B., and Richer, E. (2015). A GIS-based Method for Defining Snow Aones: Application to the Western United States, *Geocarto International,* 30(1). doi: 10.1080/10106049.2014.885089.

Oyler, J. W., Dobrowski, S. Z., Ballantyne, A. P., Klene, A. E., and Running, S. W. (2015). Artificial amplification of warming trends across the mountains of the western United States. *Geophysical Research Letters, 42*(1), 153-161. doi:10.1002/2014gl062803.

Moriasi, D. N., Arnold, J. G., Liew, M. W., Bingner, R. L., Harmel, R. D., and Veith, T. L. (2007). Model Evaluation Guidelines for Systematic Quantification of Accuracy in Watershed Simulations. *Transactions of the ASABE, 50*(3), 885-900. doi:10.13031/2013.23153.

Pederson, G. T., Gray, S. T., Ault, T., Marsh, W., Fagre, D. B., Bunn, A. G., Woodhouse, C.A., and Graumlich, L. J. (2011). Climatic Controls on the Snowmelt Hydrology of the Northern Rocky Mountains. *Journal of Climate, 24*(6), 1666-1687. doi:10.1175/2010jcli3729.1.

Pepin, N., Bradely, R. S., Diaz, H. F., Baraer, M., Caceres, E. B., Forsythe, N., Fowler, H. F., Greenwood, G., Hashmi, M. Z., Liu, X. D., Miller, J. R., Ning, L., Ohmura, A., Palazzi, E., Rangwala, I., Schoener, W., Severskiy, I., Shahgedanova, M., Wang, M. B., Williamson, S. N., and Yang, D. Q. (2015). Elevation-dependent warming in mountain regions of the world. *Nature Climate Change*, 5, 424-430.

Pielke, R. A., Sr., Stohlgren, T., Schell, L., Parton, W., Doesken, N., Redmond, K., Money, J., McKee, T., and Kittel, T.G. (2002). Problems in evaluating regional and local trends in temperature: an example from eastern Colorado, USA. *International Journal of Climatology*,*22*(4), 421-434. doi:10.1002/joc.706.

Pielke, R. A., Davey, C. A., Niyogi, D., Fall, S., Steinweg-Woods, J., Hubbard, K., Lin, X., Cai, M., Lim, Y., Li, H., Nielsen-Gammon, J., Gallo, K., Hale, R., Mahmood, R., Foster, S., McNider, R. T., and Blanken, P. (2007). Unresolved issues with the assessment of multidecadal global land surface temperature trends. *Journal of Geophysical Research,* 112(D24S08). doi:10.1029/2006jd008229

Rangwala, I., and Miller, J. R. (2012). Climate change in mountains: a review of elevation-dependent warming and its possible causes. *Climatic Change, 114*(3-4), 527-547. doi:10.1007/s10584-012-0419-3

Rangwala, I., Bardsley, T., Pescinski, M., and Miller, J. (2015). *SNOTEL* sensor upgrade has caused temperature record inhomogeneities for the Intermountain West: Implications for climate change impact assessments. *Western Water Assessment Climate Research Briefing, 11.*

Sen, P. K. (1968). Estimates of the Regression Coefficient Based on Kendall's Tau. *Journal of the American Statistical Association, 63*(324), 1379-1389. doi:10.1080/01621459.1968.10480934.

Thiel, H., 1950. A rank-invariant method of linear and polynomial regression analysis, I, II, III. *Proceedings of the Royal Netherlands Academy of Sciences,* 53, 386-392, 521-525, 1397-1412.

Venable, N. B., Fassnacht, S. R., Adyabadam, G., Tumenjargal, S., Fernández-Giménez, M., and Batbuyan, B. (2012). Does the length of station record influence the warming trend that is perceived by mongolian herders near the Khangai Mountains? *Pirineos, 167*(0), 69-86. doi:10.3989/pirineos.2012.167004

Wolter, K. (2001). Colorado forecasts, *Colorado Forecasts. National Oceanic and Atmospheric Administration,* Retrieved from https://www.esrl.noaa.gov/psd/forecasts/swcasts/MAR02.html

Yan, L., and Liu, X. (2014). Has climatic warming over the Tibetan Plateau paused or continued in recent years? *Journal of Earth, Ocean and Atmospheric Sciences 1*(1), 13-28.

APPENDIX A: DATASET SUMMARIES

Table A1. Information of the 68 long-term SNOTEL study stations in Colorado.

SNOTEL station	Station number	Latitude	Longitude	Elevation (m)
Apishapa	303	37.33062	-105.067	3048
Arrow	305	39.91550	-105.761	2950
Bear Lake	322	40.31118	-105.645	2896
Beartown	327	37.71409	-107.512	3536
Berthoud Summit	335	39.80392	-105.778	3444
Bison Lake	345	39.76487	-107.357	3316
Brumley	369	39.08766	-106.542	3231
Burro Mountain	378	39.87505	-107.599	2865
Butte	380	38.89433	-106.953	3097
Cascade	386	37.65096	-107.805	2707
Cascade #2	389	37.65800	-107.803	2719
Columbine	408	40.39480	-106.604	2792
Columbine Pass	409	38.41795	-108.382	2865
Copeland Lake	412	40.20778	-105.569	2621
Copper Mountain	415	39.48954	-106.171	3200
Crosho	426	40.16745	-107.057	2774
Culebra #2	430	37.20945	-105.200	3200
Cumbres Trestle	431	37.01878	-106.452	3054
Deadman Hill	438	40.80571	-105.770	3115
Dry Lake	457	40.53397	-106.781	2560
El Diente Peak	465	37.78617	-108.022	3109
Elk River	467	40.84781	-106.969	2652
Fremont Pass	485	39.37991	-106.197	3475
Grizzly Peak	505	39.64631	-105.870	3383
Hoosier Pass	531	39.36127	-106.060	3475
Idarado	538	37.93390	-107.676	2987
Independence Pass	542	39.07539	-106.612	3231
Joe Wright	551	40.53215	-105.887	3085
Kiln	556	39.31724	-106.615	2926
Lake Eldora	564	39.93678	-105.590	2957
Lake Irene	565	40.41432	-105.820	3261
Lily Pond	580	37.37929	-106.548	3353
Lizard Head Pass	586	37.79926	-107.924	3109
Lone Cone	589	37.89183	-108.195	2926
Lynx Pass	607	40.07806	-106.670	2707
Mc Clure Pass	618	39.12897	-107.288	2896
Middle Creek	624	37.61978	-107.035	3429

Mineral Creek	629	37.84747	-107.727	3060
Molas Lake	632	37.74932	-107.689	3200
Nast Lake	658	39.29722	-106.607	2652
Niwot	663	40.03523	-105.544	3021
North Lost Trail	669	39.07813	-107.144	2804
Park Cone	680	38.81996	-106.590	2926
Park Reservoir	682	39.04644	-107.874	3036
Phantom Valley	688	40.39937	-105.848	2752
Porphyry Creek	701	38.48884	-106.340	3280
Rabbit Ears	709	40.36783	-106.740	2865
Red Mountain Pass	713	37.89180	-107.713	3399
Ripple Creek	717	40.10812	-107.294	3152
Roach	718	40.87502	-106.046	2957
Schofield Pass	737	39.01522	-107.049	3261
Scotch Creek	739	37.64556	-108.008	2774
Slumgullion	762	37.99152	-107.204	3487
Spud Mountain	780	37.69866	-107.777	3249
Stillwater Creek	793	40.22543	-105.920	2658
Stump Lakes	797	37.47621	-107.633	3414
Summit Ranch	802	39.71796	-106.158	2865
Tower	825	40.53743	-106.677	3200
Trapper Lake	827	39.99884	-107.236	2957
University Camp	838	40.03279	-105.576	3139
Upper Rio Grande	839	37.72194	-107.260	2865
Upper San Juan	840	37.48576	-106.835	3088
Vail Mountain	842	39.61676	-106.380	3139
Vallecito	843	37.48510	-107.507	3316
Whiskey Ck	857	37.21411	-105.122	3115
Willow Creek Pass	869	40.34703	-106.094	2908
Willow Park	870	40.43254	-105.733	3261
Wolf Creek Summit	874	37.47922	-106.802	3353

Table A2a. SWE model results (NSCE and bias) during all days for all SNOTEL study stations with calibrated two model parameters T_s (°C) and α (mm/d/°C).

			NSCE				Bias			
SNOTEL Stations	Ts (°C)	α (mm/d/°C)	Calibrated	Original	H1	H2	Calibrated	Original	H1	H2
Apishapa	5.60	2.36	0.82	-0.19	0.44	0.35	0.00	-0.89	-0.56	-0.60
Arrow	6.60	1.00	0.72	0.66	0.75	0.80	0.00	-0.17	-0.08	-0.03
Bear Lake	7.20	2.30	0.94	0.85	0.88	0.95	0.00	-0.24	-0.14	-0.04
Beartown	0.50	3.20	0.92	0.86	0.86	0.69	0.00	-0.02	0.16	0.35
Berthoud Summit	1.70	3.00	0.96	0.83	0.92	0.91	0.00	-0.23	-0.08	0.10
Bison Lake	5.00	4.30	0.94	0.94	0.89	0.88	0.00	0.01	0.09	0.11
Brumley	2.50	2.80	0.95	0.72	0.92	0.93	0.00	-0.37	-0.17	0.01
Burro Mountain	5.40	3.80	0.96	0.93	0.92	0.85	0.00	-0.08	0.06	0.10
Butte	4.50	2.10	0.95	0.74	0.85	0.94	0.00	-0.28	-0.18	0.03
Cascade	2.40	2.90	0.95	0.72	0.89	0.42	0.00	-0.40	0.02	0.57
Cascade #2	2.60	3.00	0.90	0.46	0.72	0.46	0.00	-0.52	-0.13	0.47
Columbine	5.35	4.80	0.97	0.54	0.69	0.69	0.00	-0.26	-0.13	-0.14
Columbine Pass	5.35	4.18	0.92	0.89	0.96	0.93	0.00	-0.25	-0.09	0.02
Copeland Lake	4.30	2.35	0.75	-1.19	0.35	0.76	0.00	-1.22	-0.49	-0.03
Copper Mountain	3.60	3.00	0.98	0.89	0.96	0.96	0.00	-0.19	-0.06	0.04
Crosho	5.40	2.40	0.91	0.63	0.85	0.85	0.00	-0.37	-0.19	-0.19
Culebra#2	6.20	0.55	0.54	-0.21	0.06	-1.48	0.00	-0.66	-0.53	-1.18
Cumbres Trestle	5.20	2.20	0.84	0.79	0.87	0.89	0.00	-0.14	-0.07	-0.01
Deadman Hill	5.00	2.10	0.92	0.79	0.91	0.95	0.00	-0.21	-0.10	-0.01
Dry Lake	5.45	3.31	0.98	0.85	0.92	0.94	0.00	-0.18	-0.07	-0.01
El Diente Peak	0.40	3.00	0.92	0.84	0.93	0.81	0.00	-0.24	0.05	0.21
Elk River	5.00	1.50	0.87	0.75	0.85	0.90	0.00	-0.20	-0.09	-0.01
Fremont Pass	5.80	2.10	0.94	0.82	0.90	0.90	0.00	-0.14	-0.04	0.14
Grizzly Peak	4.30	3.00	0.92	0.75	0.92	0.97	0.00	-0.25	-0.12	0.03
Hoosier Pass	5.30	4.10	0.96	0.79	0.91	0.90	0.00	0.18	-0.06	0.12
Idarado	2.50	2.90	0.95	0.82	0.95	0.81	0.00	-0.29	-0.05	0.20
Independence Pass	2.30	3.00	0.93	0.73	0.88	0.92	0.01	-0.20	-0.06	0.13
Joe Wright	4.60	2.90	0.95	0.84	0.95	0.94	0.00	-0.24	-0.08	-0.02
Kiln	2.60	3.00	0.97	0.92	0.96	0.94	0.00	-0.13	0.03	0.09
Lake Eldora	5.35	3.50	0.91	0.79	0.92	0.88	0.00	-0.23	-0.06	0.10
Lake Irene	4.80	3.00	0.94	0.80	0.89	0.90	0.00	-0.05	0.05	0.17
Lily Pond	1.90	3.00	0.93	0.83	0.90	0.60	0.00	-0.25	-0.02	0.35
Lizard Head Pass	4.10	2.90	0.85	0.64	0.78	0.82	0.00	-0.27	-0.12	0.02
Lone Cone	4.10	3.00	0.88	0.67	0.84	0.90	0.00	-0.29	-0.14	0.04
Lynx Pass	4.10	2.90	0.94	0.83	0.94	0.94	0.00	-0.18	-0.03	0.04
Mc Clure Pass	6.50	2.30	0.94	0.76	0.87	0.89	0.00	-0.24	-0.13	-0.01
Middle Creek	2.10	3.00	0.94	0.86	0.95	0.94	0.00	-0.27	-0.06	-0.04
Mineral Creek	3.00	3.00	0.95	0.74	0.93	0.94	0.00	-0.32	-0.11	0.05
Molas Lake	3.10	2.50	0.91	0.88	0.93	0.84	0.00	-0.07	0.07	0.23
Nast Lake	1.50	3.15	0.89	0.88	0.88	0.80	0.00	-0.26	0.03	0.20

Niwot	4.20	1.30	0.83	0.28	0.64	0.85	0.00	-0.46	-0.24	-0.07
North Lost Trail	4.20	3.00	0.96	0.85	0.97	0.89	0.00	-0.27	-0.09	0.15
Park Cone	4.00	3.00	0.96	0.77	0.91	0.92	0.00	-0.26	-0.10	-0.03
Park Reservoir	4.60	4.30	0.96	0.94	0.94	0.83	0.00	-0.05	0.04	0.21
Phantom Valley	1.90	3.00	0.95	0.71	0.91	0.88	0.00	-0.39	-0.12	0.04
Porphyry Creek	4.40	3.90	0.88	0.67	0.86	0.28	0.00	-0.19	-0.05	0.31
Rabbit Ears	5.20	4.10	0.97	0.95	0.96	0.95	0.00	-0.13	-0.02	-0.05
Red Mountain Pass	2.30	3.10	0.97	0.79	0.85	0.82	0.00	-0.11	0.03	0.15
Ripple Creek	5.90	3.00	0.92	0.89	0.95	0.96	0.00	-0.15	-0.05	0.04
Roach	4.50	2.20	0.94	0.71	0.90	0.97	0.00	-0.31	-0.15	0.02
Schofield Pass	4.50	3.00	0.92	0.91	0.96	0.94	0.00	-0.09	0.00	0.14
Scotch Creek	1.20	3.00	0.94	0.52	0.83	0.59	0.00	-0.50	-0.11	0.42
Slumgullion	5.25	3.60	0.92	0.75	0.89	0.83	0.00	-0.20	-0.10	0.17
Spud Mountain	2.80	3.00	0.95	0.87	0.95	0.71	0.00	-0.18	0.00	0.35
Stillwater Creek	4.20	2.80	0.90	0.73	0.90	0.94	0.00	-0.27	-0.10	0.03
Stump Lakes	4.20	3.00	0.95	0.93	0.96	0.92	0.00	-0.14	-0.02	0.08
Summit Ranch	4.90	3.80	0.94	0.90	0.95	0.88	0.00	-0.18	-0.04	0.13
Tower	5.50	3.10	0.97	0.92	0.92	0.90	0.00	0.07	0.13	0.18
Trapper Lake	5.10	3.40	0.95	0.95	0.92	0.83	0.00	0.03	0.13	0.22
University Camp	4.45	2.50	0.96	0.90	0.95	0.90	0.00	-0.19	-0.03	0.06
Upper Rio Grande	2.10	3.00	0.86	0.38	0.82	0.84	0.00	-0.65	-0.29	0.01
Upper San Juan	1.30	2.80	0.96	0.90	0.95	0.93	0.00	-0.13	0.02	0.11
Vail Mountain	5.70	2.70	0.95	0.92	0.93	0.89	0.00	-0.07	0.03	0.12
Vallecito	5.20	3.00	0.91	0.84	0.87	0.85	0.00	-0.11	0.05	0.06
Whiskey Ck	5.00	3.50	0.95	0.22	0.76	0.84	0.00	-0.62	-0.32	-0.21
Willow Creek Pass	5.50	3.07	0.95	0.87	0.92	0.93	0.00	-0.16	-0.06	0.02
Willow Park	1.30	3.00	0.93	0.93	0.94	0.88	0.00	-0.18	0.01	0.13
Wolf Creek Summit	4.20	2.00	0.97	0.90	0.95	0.91	0.00	-0.13	-0.04	0.15

Table A2b. SWE model results (NSCE and bias) during snow months (October through June) only for all SNOTEL study stations with calibrated two model parameters T_s (°C) and α (mm/d/°C).

SNOTEL Stations	Ts (°C)	α (mm/d/°C)	NSCE				Bias			
			Calibrated	Original	H1	H2	Calibrated	Original	H1	H2
Apishapa	5.7	2.4	0.79	-0.35	0.38	0.23	0.00	-0.89	-0.55	-0.61
Arrow	6.6	1.0	0.64	0.58	0.70	0.75	0.00	-0.15	-0.07	-0.02
Bear Lake	7.2	2.3	0.93	0.72	0.86	0.93	0.00	-0.23	-0.14	-0.03
Beartown	0.5	3.2	0.89	0.82	0.81	0.59	0.00	-0.02	0.16	0.35
Berthoud Summit	1.7	3.0	0.95	0.77	0.89	0.87	0.00	-0.23	-0.08	0.10
Bison Lake	4.8	4.0	0.93	0.93	0.86	0.84	0.00	0.02	0.08	0.12
Brumley	2.5	2.8	0.93	0.65	0.89	0.92	0.00	-0.37	-0.17	0.01
Burro Mountain	5.7	4.2	0.94	0.91	0.90	0.82	0.00	-0.09	0.06	0.09
Butte	4.5	2.1	0.94	0.68	0.82	0.93	0.00	-0.27	-0.18	0.03
Cascade	2.4	2.9	0.94	0.67	0.88	0.33	0.00	-0.40	0.02	0.57
Cascade #2	2.6	3.0	0.89	0.40	0.68	0.39	0.00	-0.52	-0.13	0.47
Columbine	5.4	4.8	0.96	0.55	0.74	0.61	0.00	-0.21	-0.09	-0.13
Columbine Pass	5.7	4.9	0.92	0.85	0.94	0.91	0.00	-0.24	-0.08	0.01
Copeland Lake	4.3	2.4	0.71	-1.49	0.26	0.73	0.00	-1.22	-0.49	-0.02
Copper Mountain	3.6	3.0	0.97	0.86	0.95	0.95	0.00	-0.18	-0.06	0.04
Crosho	5.4	2.4	0.89	0.55	0.82	0.81	0.00	-0.37	-0.19	-0.19
Culebra#2	6.3	0.7	0.53	-0.16	0.12	-1.03	0.00	-0.50	-0.40	-0.73
Cumbres Trestle	5.2	2.2	0.79	0.74	0.84	0.87	0.00	-0.14	-0.06	-0.01
Deadman Hill	5.0	2.1	0.89	0.72	0.87	0.93	0.00	-0.19	-0.10	0.00
Dry Lake	5.5	3.3	0.98	0.80	0.90	0.92	0.00	-0.18	-0.07	-0.01
El Diente Peak	0.4	3.0	0.91	0.81	0.91	0.77	0.00	-0.24	0.05	0.21
Elk River	5.0	1.5	0.84	0.69	0.82	0.88	0.00	-0.19	-0.09	-0.01
Fremont Pass	5.8	2.1	0.92	0.78	0.87	0.86	0.00	-0.11	-0.03	0.14
Grizzly Peak	4.3	3.0	0.89	0.68	0.89	0.96	0.00	-0.24	-0.11	0.03
Hoosier Pass	5.3	4.1	0.94	0.73	0.88	0.86	0.00	-0.16	-0.06	0.12
Idarado	2.5	2.9	0.94	0.77	0.93	0.76	0.00	-0.29	-0.05	0.20
Independence Pass	2.3	3.0	0.90	0.64	0.84	0.89	0.01	-0.20	-0.06	0.13
Joe Wright	4.6	2.9	0.93	0.79	0.93	0.92	0.00	-0.22	-0.08	-0.02
Kiln	2.7	3.0	0.96	0.88	0.95	0.92	0.00	-0.15	0.02	0.08
Lake Eldora	5.4	3.5	0.88	0.74	0.90	-6.07	0.00	-0.23	-0.06	0.10
Lake Irene	4.8	2.9	0.91	0.73	0.85	0.87	0.00	-0.04	0.05	0.16
Lily Pond	1.9	3.0	0.91	0.79	0.88	0.50	0.00	-0.25	-0.02	0.35
Lizard Head Pass	4.1	2.9	0.80	0.54	0.72	0.77	0.00	-0.26	-0.12	0.02
Lone Cone	4.1	3.0	0.86	0.60	0.81	0.88	0.00	-0.28	-0.13	0.04
Lynx Pass	4.1	2.8	0.92	0.78	0.92	0.92	0.00	-0.19	-0.04	0.04
Mc Clure Pass	6.6	2.4	0.93	0.70	0.84	0.87	0.00	-0.25	-0.12	0.00
Middle Creek	2.1	3.0	0.92	0.81	0.93	0.92	0.00	-0.26	-0.06	-0.04
Mineral Creek	3.0	3.0	0.94	0.68	0.91	0.93	0.00	-0.32	-0.11	0.05

Molas Lake	3.1	2.5	0.89	0.85	0.91	0.80	0.00	-0.06	0.07	0.23
Nast Lake	1.5	3.2	0.88	0.86	0.86	0.76	0.00	-0.26	0.03	0.87
Niwot	4.2	1.3	0.77	0.14	0.56	-4.31	0.00	-0.44	-0.23	-0.07
North Lost Trail	4.2	3.0	0.95	0.81	0.96	0.86	0.00	-0.27	-0.09	0.15
Park Cone	4.0	3.0	0.95	0.72	0.89	0.51	0.00	-0.26	-0.09	0.20
Park Reservoir	4.6	4.2	0.94	0.91	0.92	0.78	0.00	-0.05	0.04	0.21
Phantom Valley	1.9	3.0	0.94	0.63	0.88	0.85	0.01	-0.39	-0.12	0.04
Porphyry Creek	4.4	3.7	0.84	0.55	0.80	0.06	0.00	0.17	-0.05	0.30
Rabbit Ears	5.2	4.1	0.97	0.94	0.94	0.94	0.00	-0.12	-0.02	0.88
Red Mountain Pass	2.3	3.1	0.96	0.72	0.80	0.76	0.00	-0.11	0.03	0.15
Ripple Creek	5.9	3.0	0.90	0.86	0.94	0.95	0.00	-0.14	-0.04	0.05
Roach	4.5	2.2	0.92	0.61	0.87	0.95	0.00	-0.31	-0.15	0.02
Schofield Pass	4.7	3.0	0.88	0.87	0.94	0.92	0.00	-0.08	-0.01	0.13
Scotch Creek	1.2	3.0	0.92	0.43	0.81	0.51	0.00	-0.50	-0.11	0.43
Slumgullion	5.3	3.6	0.89	0.65	0.85	0.77	0.00	-0.19	-0.10	0.17
Spud Mountain	2.8	3.0	0.93	0.84	0.94	0.63	0.00	-0.18	0.00	0.35
Stillwater Creek	4.2	2.8	0.88	0.68	0.88	0.93	0.00	-0.27	-0.10	0.03
Stump Lakes	4.2	3.0	0.93	0.91	0.95	0.89	0.00	-0.14	-0.02	0.08
Summit Ranch	4.9	3.8	0.93	0.87	0.93	0.84	0.00	-0.18	-0.04	0.13
Tower	5.7	3.1	0.96	0.89	0.89	0.85	0.00	0.07	0.13	0.17
Trapper Lake	5.1	3.4	0.94	0.93	0.90	0.78	0.00	0.03	0.13	0.22
University Camp	4.5	2.5	0.94	0.88	0.93	0.87	0.00	-0.18	-0.03	0.06
Upper Rio Grande	2.1	3.0	0.83	0.28	0.79	0.82	0.00	-0.65	-0.29	0.01
Upper San Juan	1.3	2.8	0.95	0.87	0.94	0.90	0.00	-0.12	0.03	0.11
Vail Mountain	5.7	2.7	0.94	0.90	0.90	0.85	0.00	-0.07	0.04	0.12
Vallecito	5.2	3.0	0.89	0.80	0.84	0.82	0.00	-0.10	0.05	0.06
Whiskey Ck	5.0	3.5	0.94	0.04	0.71	0.80	0.00	-0.62	-0.32	-0.21
Willow Creek Pass	5.5	2.9	0.93	0.81	0.89	0.92	0.00	-0.16	-0.07	0.02
Willow Park	1.3	3.0	0.91	0.84	0.92	0.84	0.00	-0.17	0.01	0.13
Wolf Creek Summit	4.3	2.0	0.96	0.90	0.95	0.88	0.00	-0.11	-0.03	0.14

Table A2c. SWE model results (NSCE and bias) during melt months only (March through May) for all SNOTEL study stations with calibrated two model parameters T_s (°C) and α (mm/d/°C).

			NSCE				Bias			
SNOTEL Stations	Ts (°C)	α (mm/d/°C)	Calibrated	Original	H1	H2	Calibrated	Original	H1	H2
Apishapa	5.6	3.1	0.74	-0.58	0.45	0.26	0.00	-1.08	-0.55	-0.66
Arrow	6.7	1.0	0.44	0.36	0.50	0.57	0.00	-0.09	-0.03	-0.01
Bear Lake	7.2	1.8	0.74	0.54	0.72	0.85	0.00	-0.14	-0.08	0.00
Beartown	0.4	3.6	0.81	0.65	0.48	-0.18	0.00	0.09	0.23	0.42
Berthoud Summit	2.0	3.0	0.88	0.45	0.69	0.56	0.00	-0.15	-0.04	0.11
Bison Lake	4.5	4.0	0.84	0.80	0.55	0.47	0.00	0.05	0.12	0.15
Brumley	2.5	3.0	0.88	0.38	0.84	0.85	0.00	-0.38	-0.14	0.05
Burro Mountain	5.0	3.0	0.94	0.87	0.84	0.70	0.00	-0.03	0.11	0.19
Butte	4.5	2.0	0.85	0.48	0.69	0.87	0.00	-0.28	-0.18	0.05
Cascade	2.4	3.0	0.92	0.51	0.86	0.06	0.00	-0.50	0.08	0.74
Cascade #2	2.1	3.0	0.84	0.19	0.70	0.23	0.00	-0.74	-0.07	0.66
Columbine	5.3	4.3	0.90	0.31	0.64	0.32	0.00	-0.20	-0.06	-0.11
Columbine Pass	5.0	4.0	0.84	0.87	0.94	0.85	0.00	-0.18	0.03	0.16
Copeland Lake	3.8	2.3	0.64	-2.46	0.15	0.63	0.00	-1.93	-0.66	0.11
Copper Mountain	3.8	3.0	0.92	0.66	0.88	0.86	0.00	-0.18	-0.05	0.05
Crosho	5.4	2.5	0.83	0.25	0.72	0.70	0.00	-0.46	-0.22	-0.22
Culebra#2	6.2	1.0	0.45	-0.21	0.10	-1.12	0.00	-0.42	-0.32	-0.60
Cumbres Trestle	4.7	2.0	0.65	0.64	0.76	0.78	0.00	-0.11	-0.03	0.03
Deadman Hill	5.5	2.1	0.82	0.51	0.74	0.84	0.00	-0.12	-0.07	-0.01
Dry Lake	5.5	3.1	0.96	0.58	0.79	0.87	0.00	-0.21	-0.09	-0.01
El Diente Peak	0.7	3.0	0.85	0.62	0.86	0.64	0.00	-0.29	0.05	0.21
Elk River	4.8	1.5	0.77	0.47	0.67	0.77	0.00	-0.20	-0.09	0.00
Fremont Pass	6.6	1.0	0.81	-11.23	-0.31	0.78	0.00	-0.62	-0.12	0.06
Grizzly Peak	4.3	3.9	0.87	0.55	0.85	0.81	0.00	-0.18	-0.06	0.09
Hoosier Pass	5.3	4.0	0.86	0.44	0.70	0.59	0.00	0.15	-0.05	0.14
Idarado	2.5	2.8	0.88	0.57	0.90	0.60	0.00	-0.33	-0.03	0.26
Independence Pass	1.8	3.0	0.85	0.39	0.74	0.74	0.00	-0.20	-0.04	0.15
Joe Wright	5.0	3.0	0.87	0.57	0.83	0.75	0.00	-0.17	-0.07	-0.02
Kiln	2.7	3.0	0.93	0.78	0.92	0.86	0.00	-0.18	0.04	0.12
Lake Eldora	5.9	4.2	0.84	0.57	0.79	-3.45	0.00	-0.25	-0.10	0.14
Lake Irene	5.0	2.0	0.79	0.45	0.56	0.60	0.00	0.03	0.06	0.06
Lily Pond	1.9	3.1	0.85	0.68	0.77	-0.05	0.00	-0.20	0.04	0.45
Lizard Head Pass	4.1	3.5	0.70	0.35	0.57	0.53	0.00	-0.17	-0.04	0.11
Lone Cone	3.9	3.0	0.75	0.32	0.70	0.80	0.00	-0.40	-0.18	0.05
Lynx Pass	4.1	3.1	0.86	0.64	0.86	0.84	0.00	-0.20	0.01	0.11
Mc Clure Pass	6.4	2.1	0.85	0.58	0.75	0.81	0.00	-0.26	-0.13	0.01
Middle Creek	1.9	3.0	0.79	0.74	0.89	0.86	0.00	-0.21	-0.03	-0.02
Mineral Creek	2.9	3.1	0.87	0.51	0.87	0.84	0.00	-0.31	-0.07	0.11
Molas Lake	3.2	2.9	0.81	0.79	0.81	0.51	0.00	0.00	0.14	0.29
Nast Lake	2.0	3.1	0.88	0.74	0.91	0.75	0.00	-0.31	0.05	0.26

Niwot	3.7	1.1	0.55	-0.30	0.28	-1.43	0.00	-0.41	-0.25	-0.10
North Lost Trail	4.4	3.0	0.90	0.68	0.93	0.75	0.00	-0.27	-0.07	0.23
Park Cone	4.2	2.8	0.90	0.41	0.79	0.29	0.00	-0.38	-0.15	0.15
Park Reservoir	4.7	3.6	0.92	0.83	0.84	0.52	0.00	-0.01	0.05	0.21
Phantom Valley	2.3	3.0	0.94	0.24	0.79	0.77	0.01	-0.51	-0.16	0.11
Porphyry Creek	3.5	3.0	0.68	0.27	0.64	-1.01	0.00	-0.18	-0.06	0.30
Rabbit Ears	5.2	3.4	0.94	0.82	0.91	0.89	0.00	-0.10	-0.01	-0.02
Red Mountain Pass	2.3	3.3	0.87	0.32	0.35	0.10	0.00	-0.01	0.10	0.21
Ripple Creek	5.9	2.5	0.82	0.64	0.81	0.85	0.00	-0.10	-0.04	0.04
Roach	4.5	2.1	0.89	0.34	0.78	0.89	0.00	-0.24	-0.13	0.03
Schofield Pass	5.4	3.0	0.76	0.74	0.87	0.84	0.00	-0.04	0.02	0.10
Scotch Creek	1.1	3.0	0.87	0.11	0.68	0.30	0.00	-0.67	-0.15	0.55
Slumgullion	4.7	3.5	0.74	0.58	0.82	0.15	0.00	-0.12	-0.03	0.27
Spud Mountain	2.5	3.0	0.87	0.73	0.88	0.18	0.00	-0.17	0.02	0.40
Stillwater Creek	4.1	3.1	0.83	0.53	0.86	0.86	0.00	-0.36	-0.06	0.12
Stump Lakes	4.3	3.0	0.84	0.87	0.91	0.79	0.00	-0.09	0.00	0.11
Summit Ranch	5.0	3.8	0.89	0.73	0.90	0.66	0.01	-0.17	0.00	0.22
Tower	6.3	3.1	0.93	0.51	0.43	0.28	0.00	0.11	0.13	0.16
Trapper Lake	5.2	3.0	0.89	0.85	0.80	0.51	0.00	0.03	0.13	0.23
University Camp	4.5	2.3	0.79	0.78	0.87	0.70	0.00	-0.13	-0.02	0.08
Upper Rio Grande	2.4	2.9	0.78	-0.27	0.61	0.84	0.00	-0.94	-0.45	0.00
Upper San Juan	1.4	2.8	0.93	0.85	0.89	0.80	0.00	-0.08	0.05	0.13
Vail Mountain	5.8	2.8	0.89	0.80	0.71	0.45	0.00	-0.02	0.08	0.17
Vallecito	4.9	3.0	0.77	0.68	0.72	0.69	0.00	-0.04	0.10	0.11
Whiskey Ck	4.8	3.1	0.90	-0.59	0.52	0.68	0.00	-0.67	-0.30	-0.18
Willow Creek Pass	5.9	2.8	0.86	0.66	0.84	0.85	0.00	-0.12	-0.03	0.04
Willow Park	1.6	3.0	0.82	0.73	0.81	0.59	0.00	-0.14	0.03	0.15
Wolf Creek Summit	4.5	1.9	0.94	0.90	0.94	0.68	0.00	-0.05	0.00	0.14

Table A3. SNOTEL station with the homogenization method that best improves SWE model performance.

	Greatest NSCE			Smallest Bias		
SNOTEL Stations	Original	H1	H2	Original	H1	H2
Apishapa		✓			✓	
Arrow			✓			✓
Bear Lake			✓			✓
Beartown	✓			✓		
Berthoud Summit		✓			✓	
Bison Lake	✓			✓		
Brumley			✓			✓
Burro Mountain	✓				✓	
Butte			✓			✓
Cascade		✓			✓	
Cascade #2		✓			✓	
Columbine		✓			✓	
Columbine Pass		✓				✓
Copeland Lake			✓			✓
Copper Mountain			✓			✓
Crosho		✓				✓
Culebra#2		✓			✓	
Cumbres Trestle			✓			✓
Deadman Hill			✓			✓
Dry Lake			✓			✓
El Diente Peak		✓			✓	
Elk River			✓			✓
Fremont Pass			✓		✓	
Grizzly Peak			✓			✓
Hoosier Pass		✓			✓	
Idarado		✓			✓	
Independence Pass			✓		✓	
Joe Wright		✓				✓
Kiln		✓			✓	
Lake Eldora		✓			✓	
Lake Irene			✓	✓		
Lily Pond		✓			✓	
Lizard Head Pass			✓			✓
Lone Cone			✓			✓
Lynx Pass		✓			✓	
Mc Clure Pass			✓			✓
Middle Creek		✓				✓
Mineral Creek			✓			✓
Molas Lake		✓		✓		

Nast Lake		✓			✓	
Niwot			✓			✓
North Lost Trail		✓			✓	
Park Cone			✓			✓
Park Reservoir		✓			✓	
Phantom Valley		✓				✓
Porphyry Creek		✓			✓	
Rabbit Ears		✓			✓	
Red Mountain Pass		✓			✓	
Ripple Creek			✓			✓
Roach			✓			✓
Schofield Pass		✓			✓	
Scotch Creek		✓			✓	
Slumgullion		✓			✓	
Spud Mountain		✓			✓	
Stillwater Creek			✓			✓
Stump Lakes		✓			✓	
Summit Ranch		✓			✓	
Tower	✓			✓		
Trapper Lake	✓			✓		
University Camp		✓			✓	
Upper Rio Grande			✓			✓
Upper San Juan		✓			✓	
Vail Mountain		✓			✓	
Vallecito		✓			✓	
Whiskey Ck			✓			✓
Willow Creek Pass			✓			✓
Willow Park		✓			✓	
Wolf Creek Summit		✓			✓	

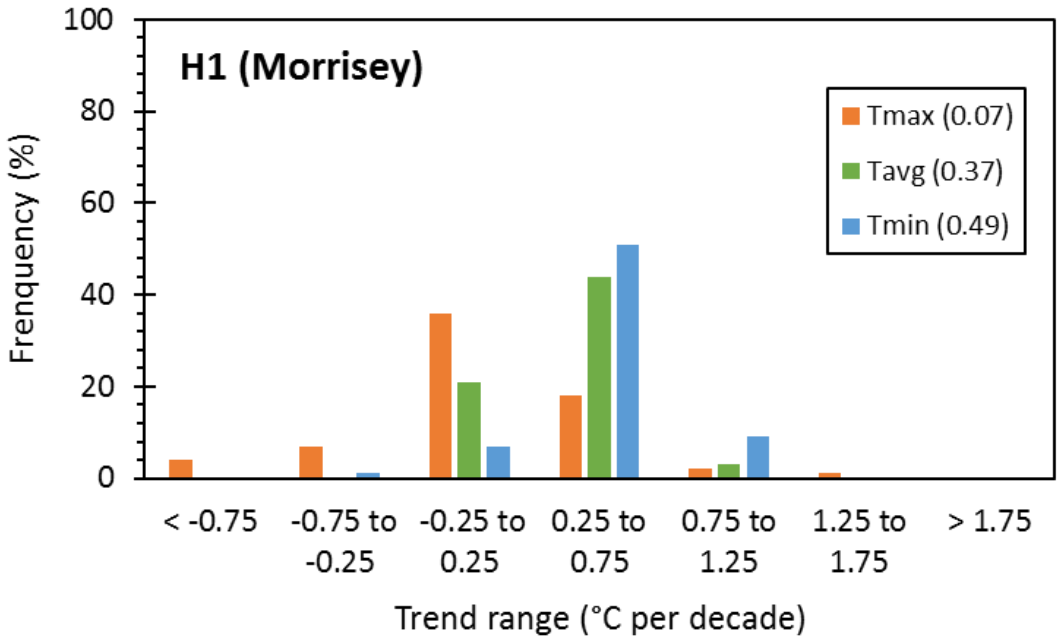

Figure A1. Histogram of H1 (Morrisey) from 1980s to 2015.